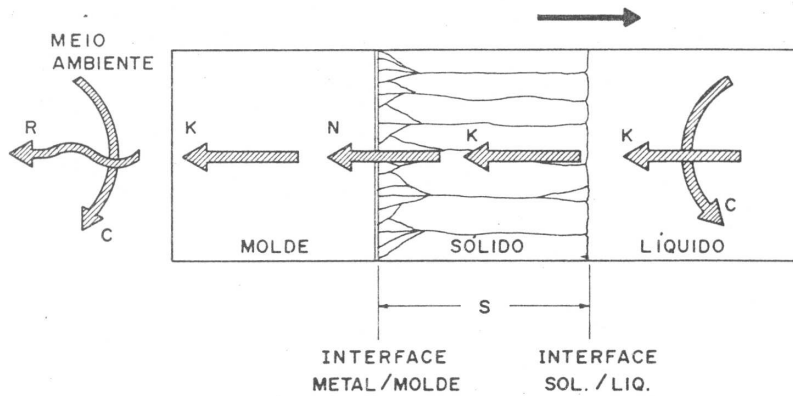




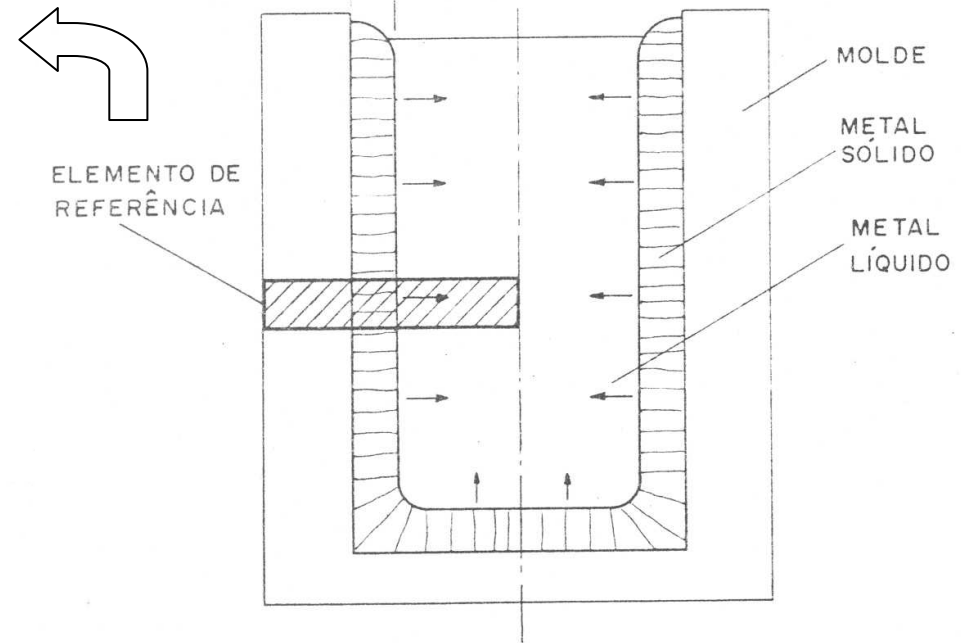
Fundição

- Projetos de Moldes

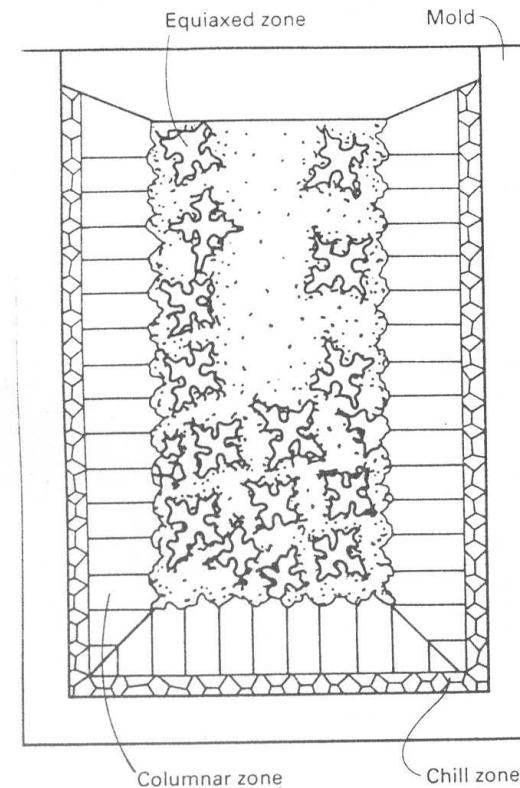
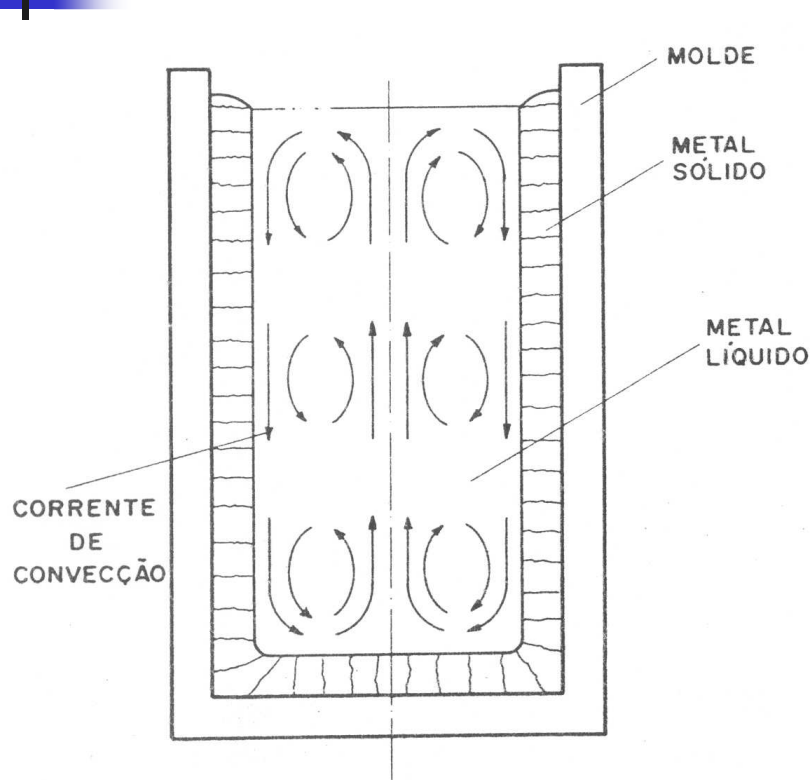
Fluxo de calor e direção de crescimento



K = CONDUÇÃO
N = TRANSFERÊNCIA NEWTONIANA
C = CONVECÇÃO
R = RADIAÇÃO



Formação da macroestrutura



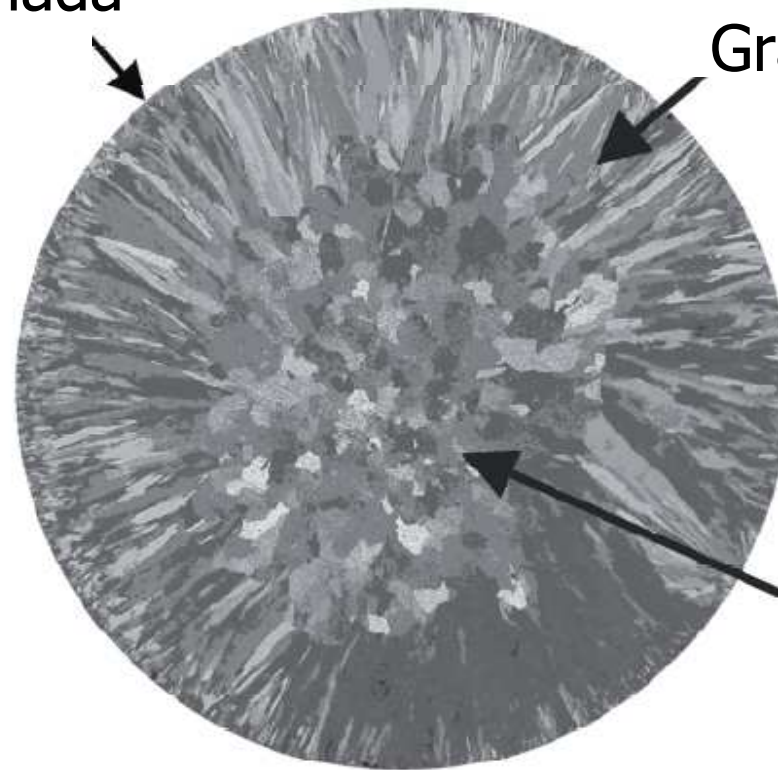
Filme

Fig. 11 Schematic of microstructure zone formation in castings. Directional solidification conditions give rise to a columnar zone, while an equiaxed zone is formed at the center where the liquid is undercooled.

Macroestrutura

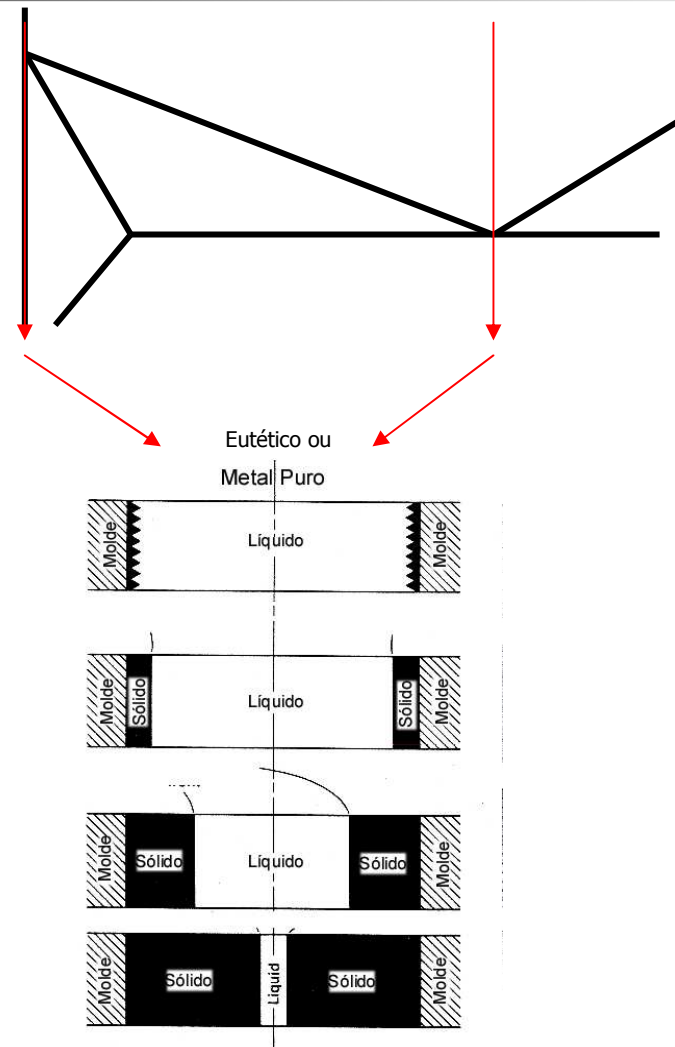
Zona Coquilhada

Grão Colunares

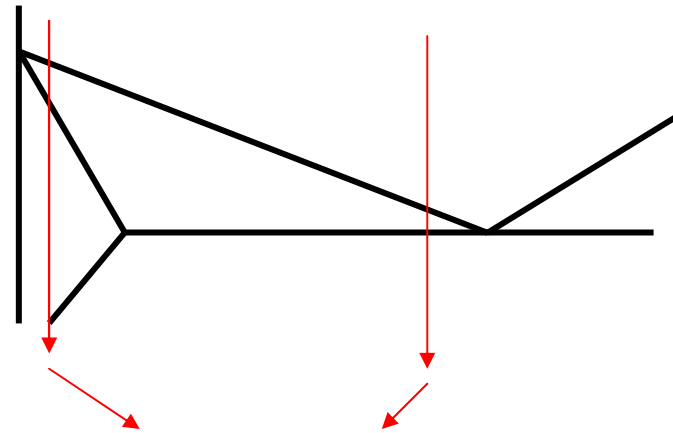


Grão Equiaxiais

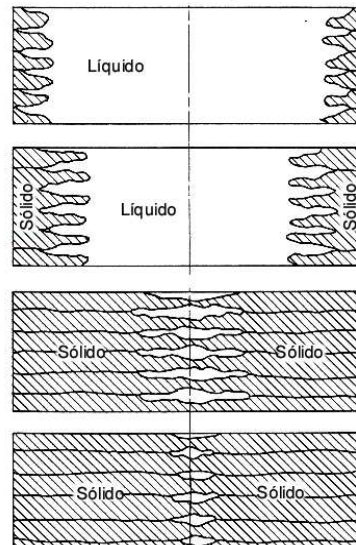
Intervalo de Solidificação e a macroestrutura



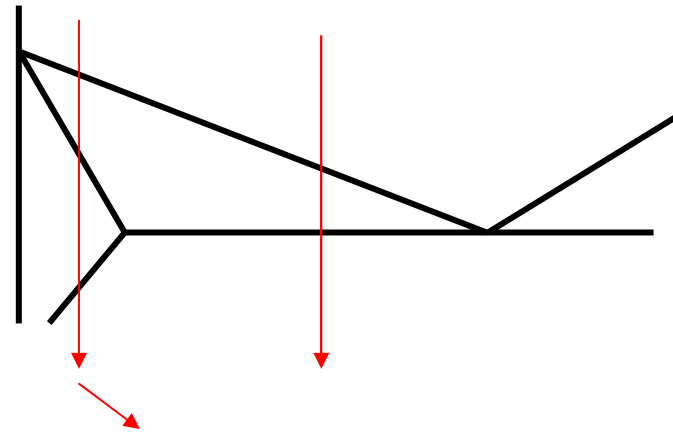
Intervalo de Solidificação e a macroestrutura



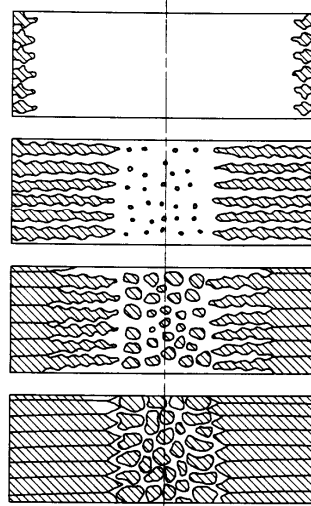
Liga com curto intervalo de solidificação



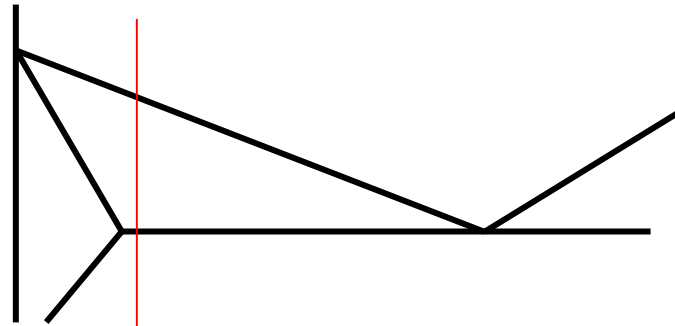
Intervalo de Solidificação e a macroestrutura



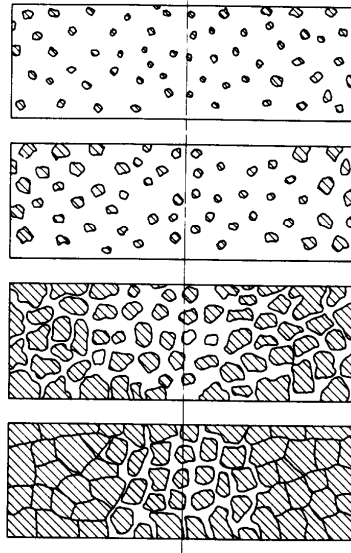
Liga com intervalo de solidificação intermediário



Intervalo de Solidificação e a macroestrutura



Liga com longo
intervalo de solidificação



Contração na Solidificação

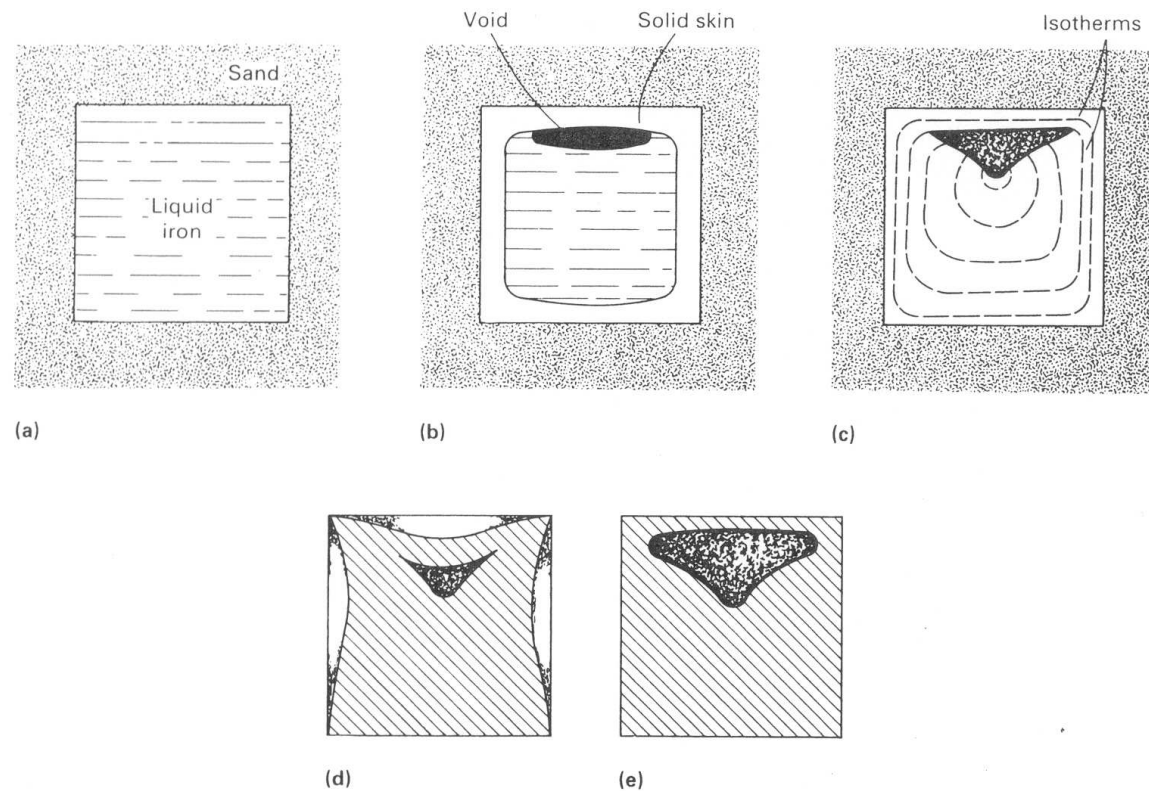


Fig. 2 Schematic of sequence of solidification shrinkage in an iron cube. (a) Initial liquid metal. (b) Solid skin and formation of shrinkage void. (c) Internal shrinkage. (d) Internal shrinkage plus dishing. (e) Surface puncture



Contração na solidificação

<i>Metal</i>	<i>Crystal structure</i>	<i>Melting point</i> °C	<i>Liquid density</i> (kg/m ³)	<i>Solid density</i> (kg/m ³)	<i>Volume change</i> (%)	<i>Ref.</i>
Al	fcc	660	2368	2550	7.14	1
Au	fcc	1063	17 380	18 280	5.47	1
Co	fcc	1495	7750	8180	5.26	1
Cu	fcc	1083	7938	8382	5.30	1
Ni	fcc	1453	7790	8210	5.11	1
Pb	fcc	327	10 665	11 020	3.22	1
Fe	bcc	1536	7035	7265	3.16	1
Li	bcc	181	528	–	2.74	4,5
Na	bcc	97	927	–	2.6	4,5
K	bcc	64	827	–	2.54	4,5
Rb	bcc	39	1437	–	2.3	4,5
Cs	bcc	29	1854	–	2.6	4,5
Tl	bcc	303	11 200	–	2.2	2
Cd	hcp	321	7998	–	4.00	2
Mg	hcp	651	1590	1655	4.10	3
Zn	hcp	420	6577	–	4.08	2
Ce	hcp	787	6668	6646	–0.33	1
In	fcc	156	7017	–	1.98	2
Sn	tetrag	232	6986	7166	2.51	1
Bi	rhomb	271	10 034	9701	–3.32	1
Sb	rhomb	631	6493	6535	0.64	1
Si	diam	1410	2525	–	–2.9	2

References: 1, Wray (1976); 2, Lucas (quoted by Wray, 1976); 3, This book; 4, Iida and Guthrie (1988); 5, Brandes (1983).



O módulo de resfriamento

- Módulo de Resfriamento

$$MR = \frac{Volume}{Superfície}$$

- Tempo de Solidificação

$$TS = c.(MR)^n \quad \blacksquare \quad 1,5 < n < 2$$

- Exemplos:
 - Calcular p/ Esfera, Chapa, Cubo, Cilindro
 - Como maximizar MR p/ Cilindro?
 - Comparar
 - MR em geometrias mais complexas



Massalotes

- Usados em fundidos, ou parte de fundidos, com MR elevado
- Geralmente desnecessários para fundidos de paredes finas (< 6 mm)
- $MR_m > 1,2.MR_f$

Massalotes

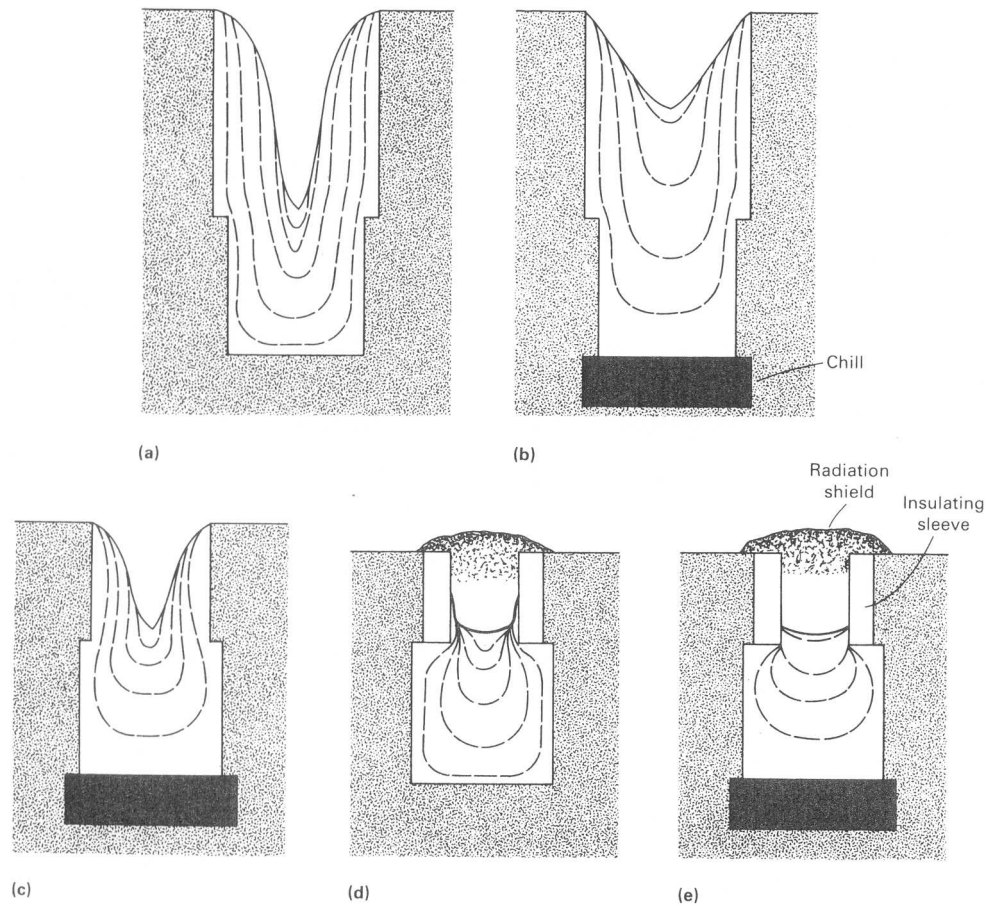


Fig. 3 Methods of controlling shrinkage in an iron cube to reduce riser size. (a) Open-top riser. (b) Open-top riser plus chill. (c) Small open-top riser plus chill. (d) Insulated riser. (e) Insulated riser plus chill

Eficiência de massalotes

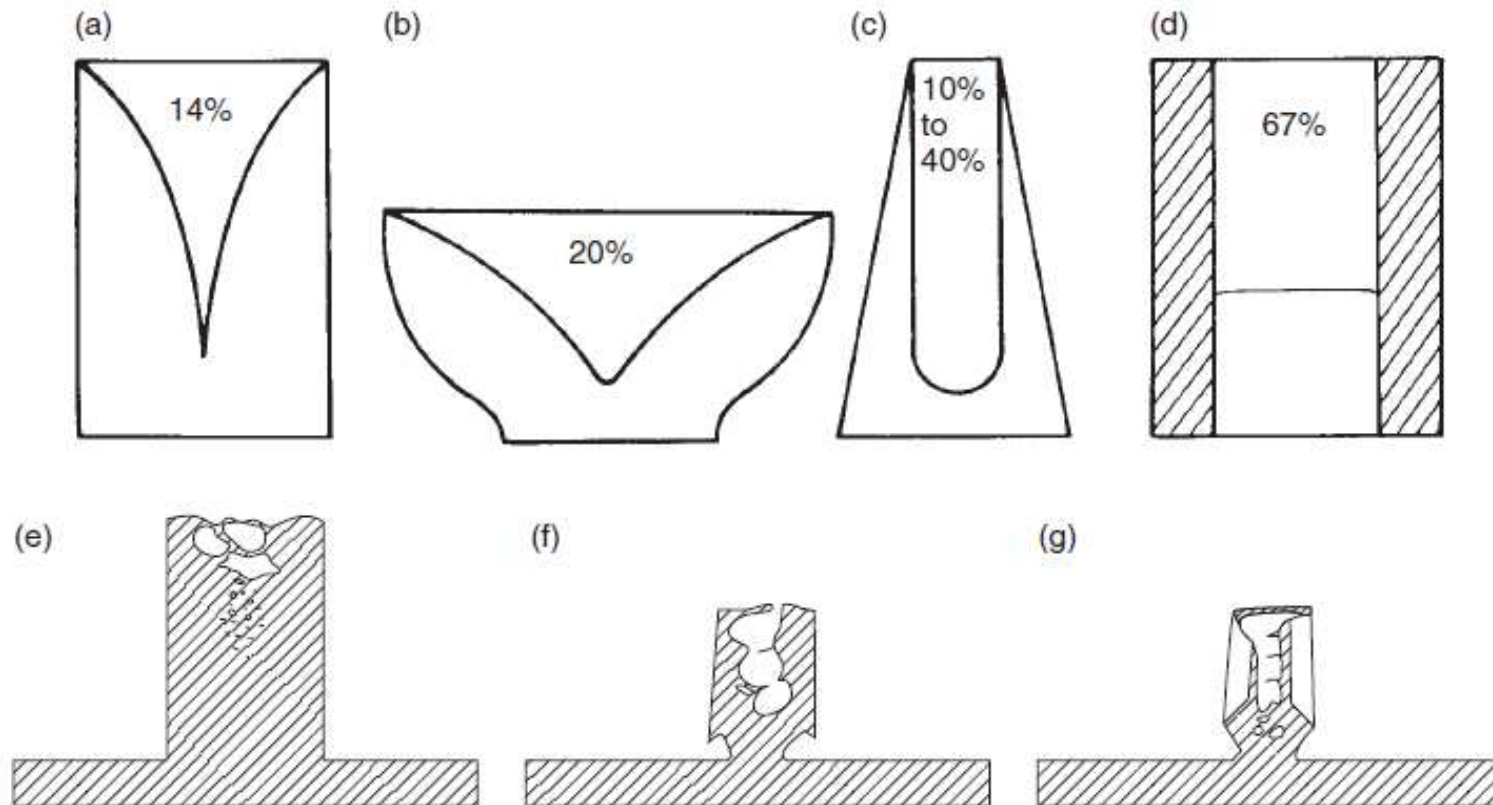


Figure 6.5 Metal utilization of feeders of various forms moulded in sand. The (a) cylindrical and (b) hemispherical heads have been treated with normal feeding compounds; (c) efficiency of the reverse taper heads depends on detailed geometry (Heine, 1982, 1983); (d) exothermic sleeve (Beeley, 1972). Metal utilization for ductile iron plates with (e) cylindrical sand feeder; (f) insulating feeder; and (g) cruciform exothermic feeder (after Foseco 1988).



Volume do Massalote

- $V_m = \alpha \cdot V_p / (e - \alpha)$
- Exemplos para massalote cilíndrico com $H = 1,5D$ ($e = 14\%$):
 - Ligas de Al: $V_m = V_p$
 - Aços: $V_m = 0,4 V_p$

Posicionamento de massalotes

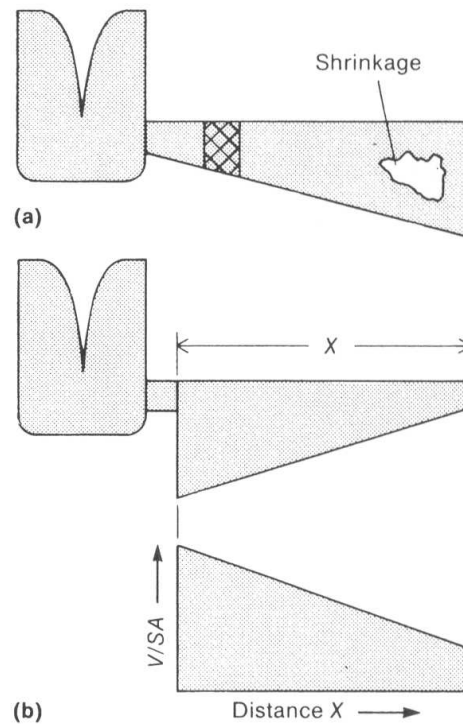


Fig. 3 Casting design and solidification of a simple wedge. (a) Riser placed at narrow end of wedge; shrinkage occurs at wide end. The crosshatched region represents the approximate area of the casting where solidification is first complete, thus cutting off the feeding path of the casting. (b) Correct riser placement. V/SA is the volume-to-surface-area ratio (casting modulus).

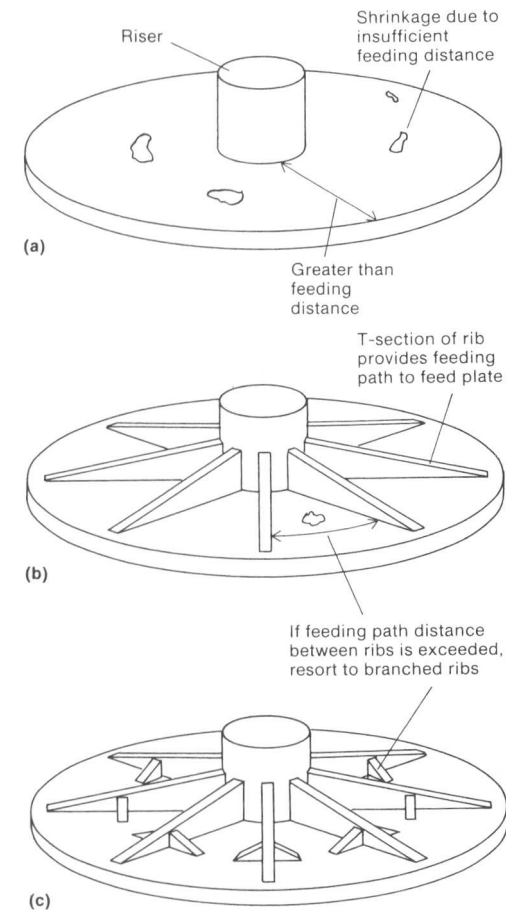
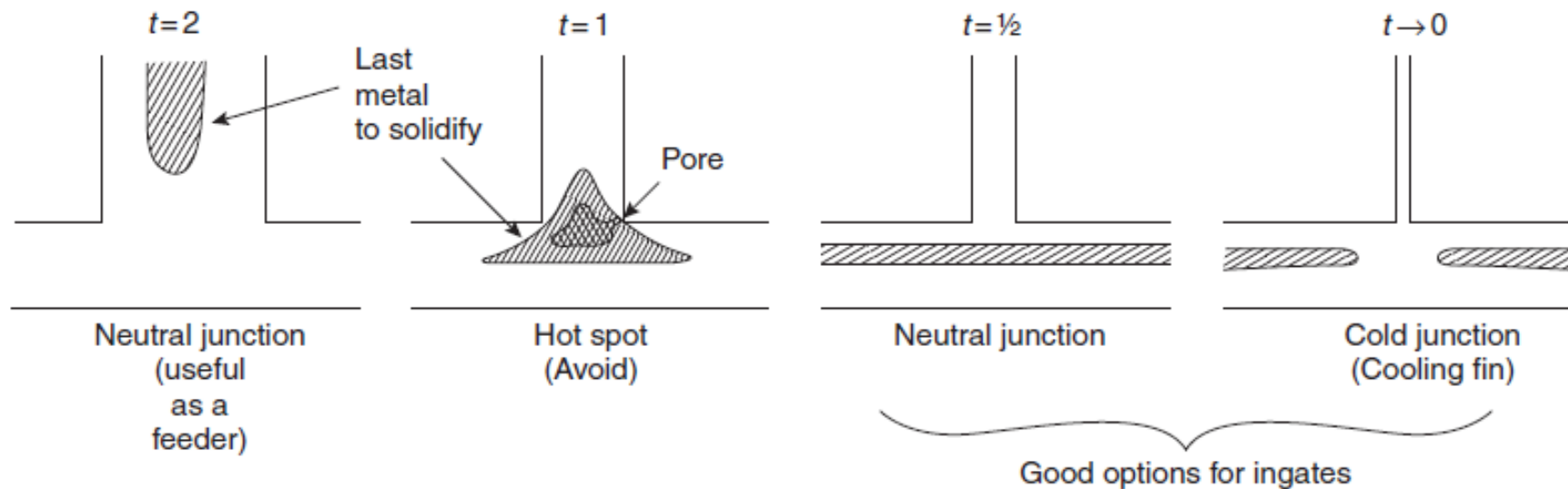


Fig. 16 Feeding path design considerations. (a) Circular flat plate with a single riser. (b) Addition of wedge-shaped ribs to ensure proper solidification. (c) Branched ribs to overcome feeding problems at the circumference of the plate

Ligação do massalote à peça



t = razão entre as espessuras

Posicionamento de Massalotes (direcionando a solidificação)

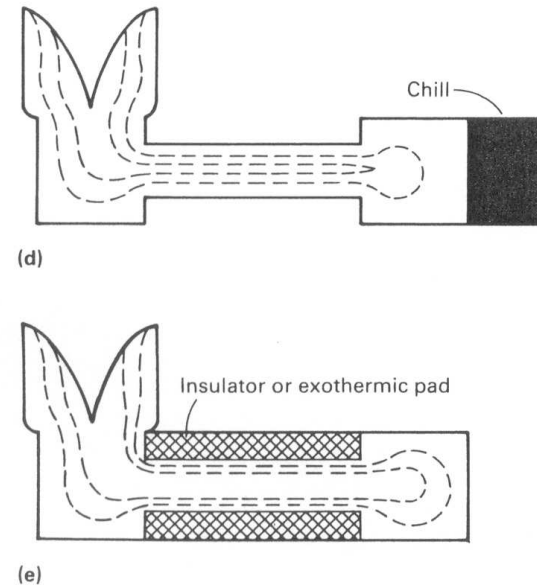
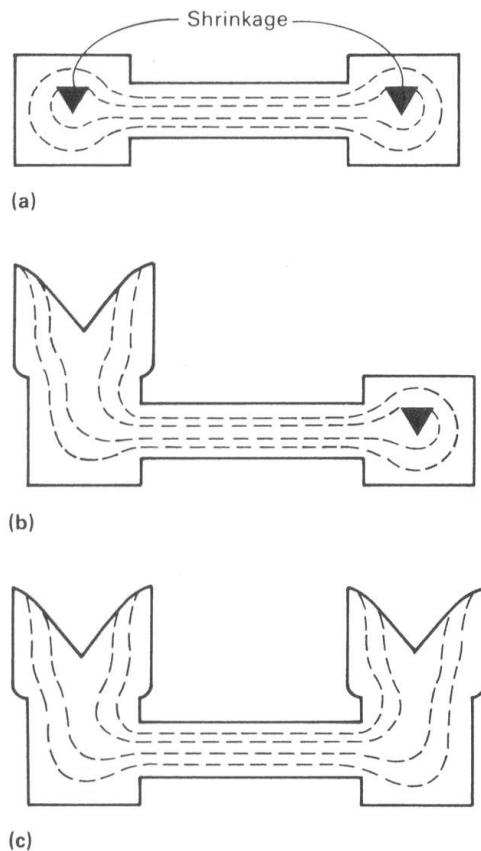


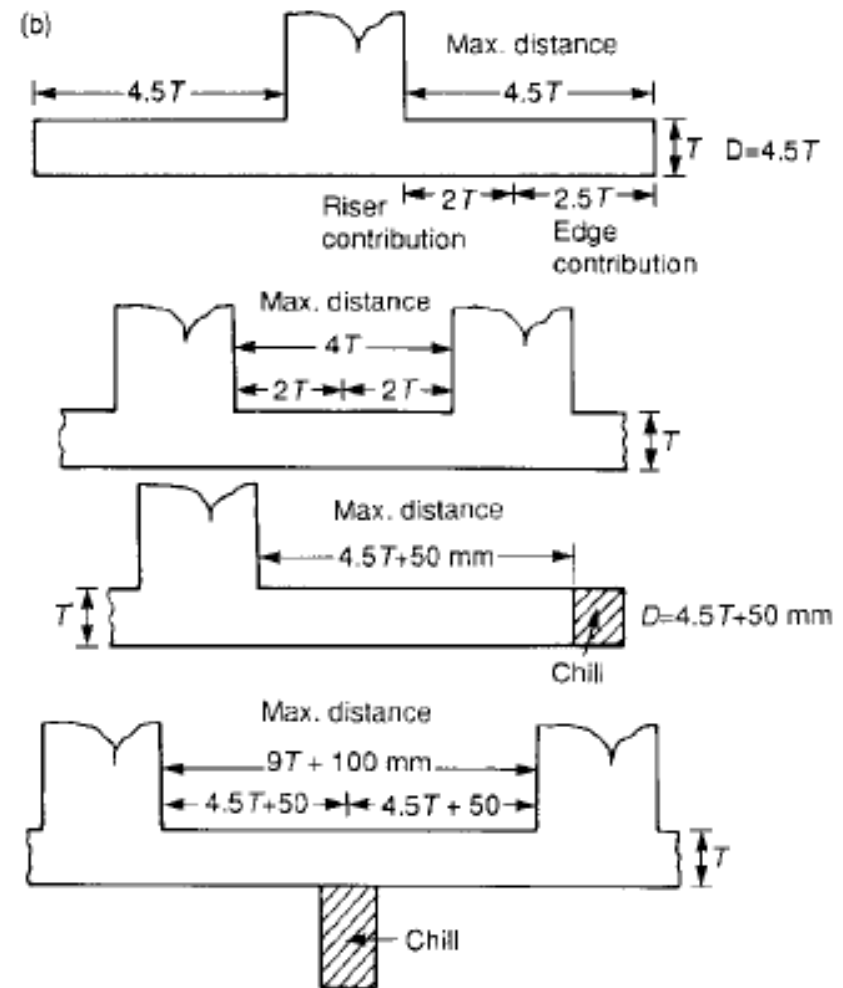
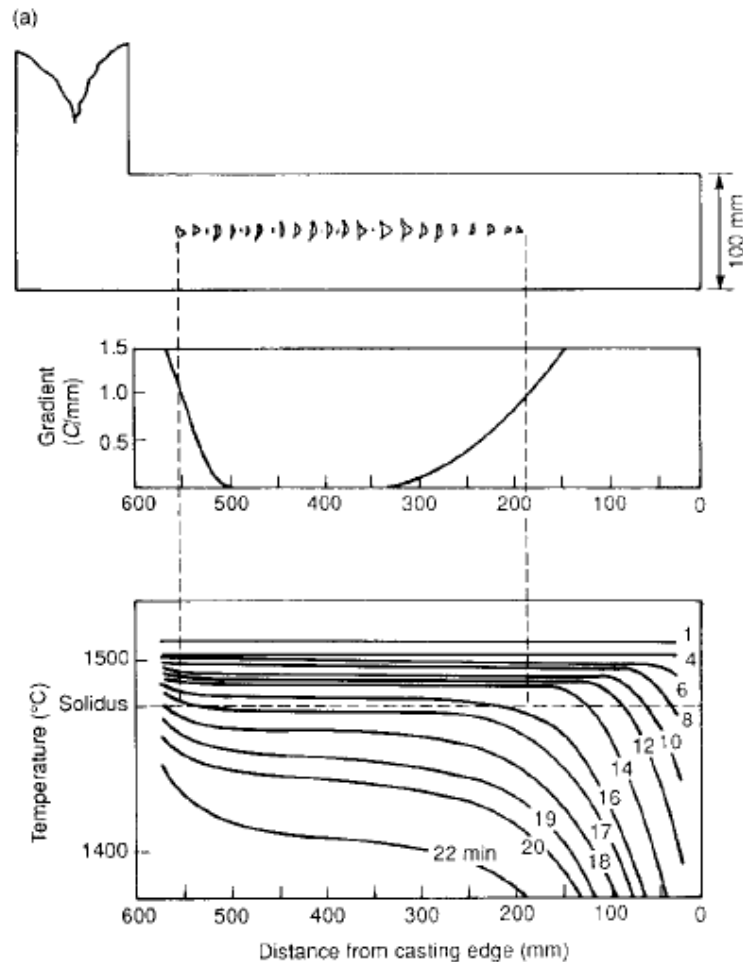
Fig. 16 Risering of isolated heavy sections joined by a thinner section to minimize shrinkage and number of risers. (a) Workpiece with no risers. (b) Riser added to one side. (c) Risers located on both ends. (d) Chill applied to one end and riser to other end. (e) Riser used on one end and insulator or exothermic pad on opposite end



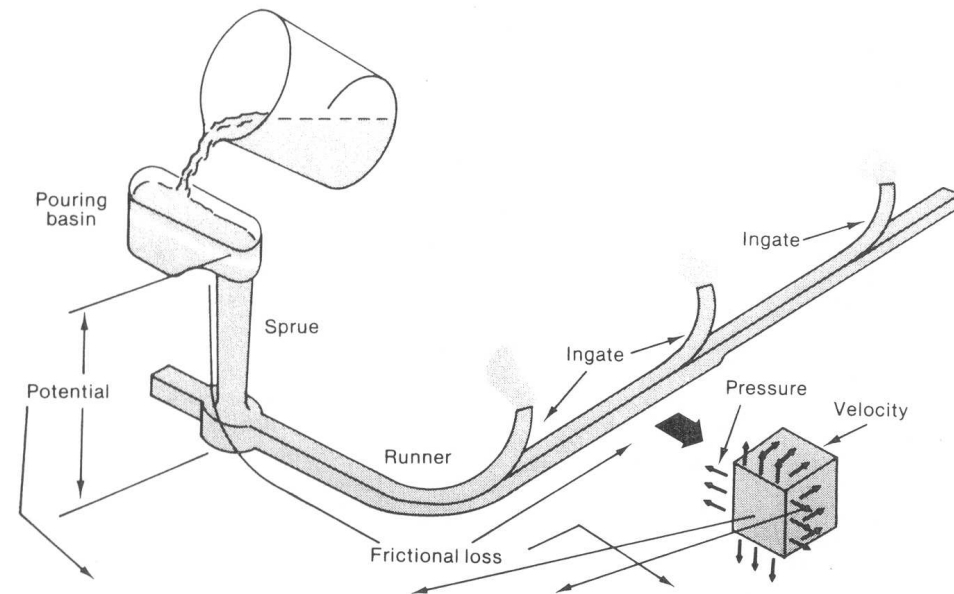
Exemplos

- Simulações em Excel

Mais de um massalote



Sistema de preenchimento



Potential head (wZ) + Pressure head (wPv) + Velocity head ($wV^2/2g$) + Frictional loss of head (wF) = Constant (K)

Fig. 2 Schematic illustrating the application of Bernoulli's theorem to a gating system. Source: Ref 1

Principal função:

•Evitar turbulência superficial

- Manter avanço contínuo da superfície líquida
- Evitar efeito "cascata" e a incorporação de bolhas
- Controlar a velocidade e evitar projeção de metal

Medidas de fluidez

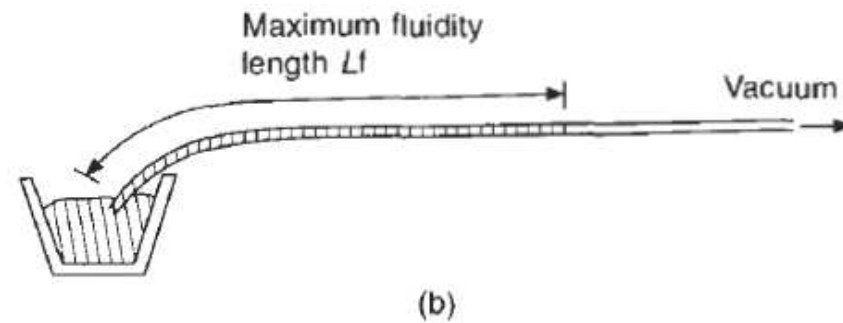
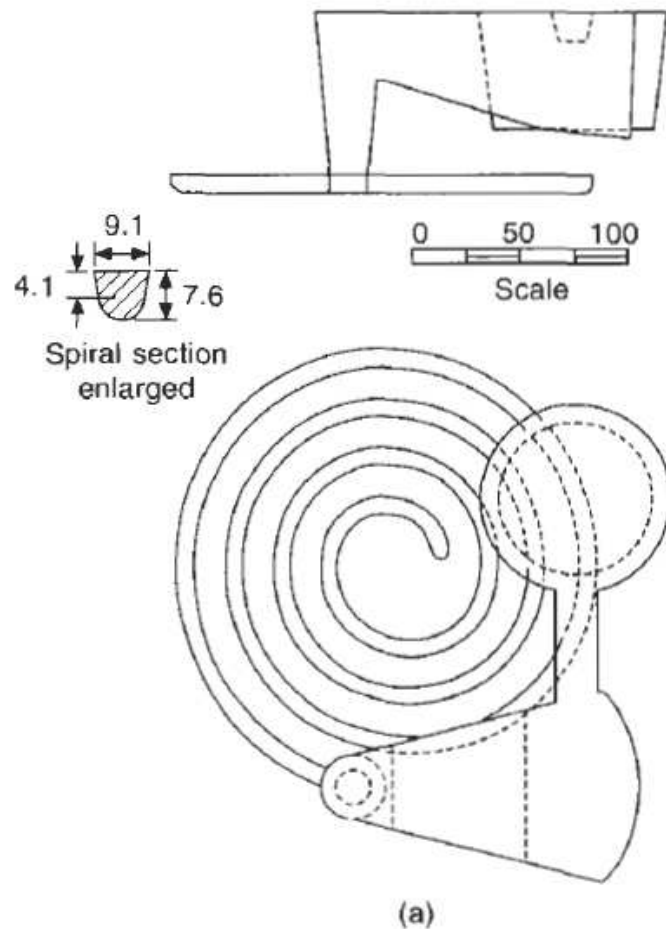


Figure 3.2 Typical fluidity tests for (a) foundry and (b) laboratory use.

Influência do tipo de liga na fluidez do metal

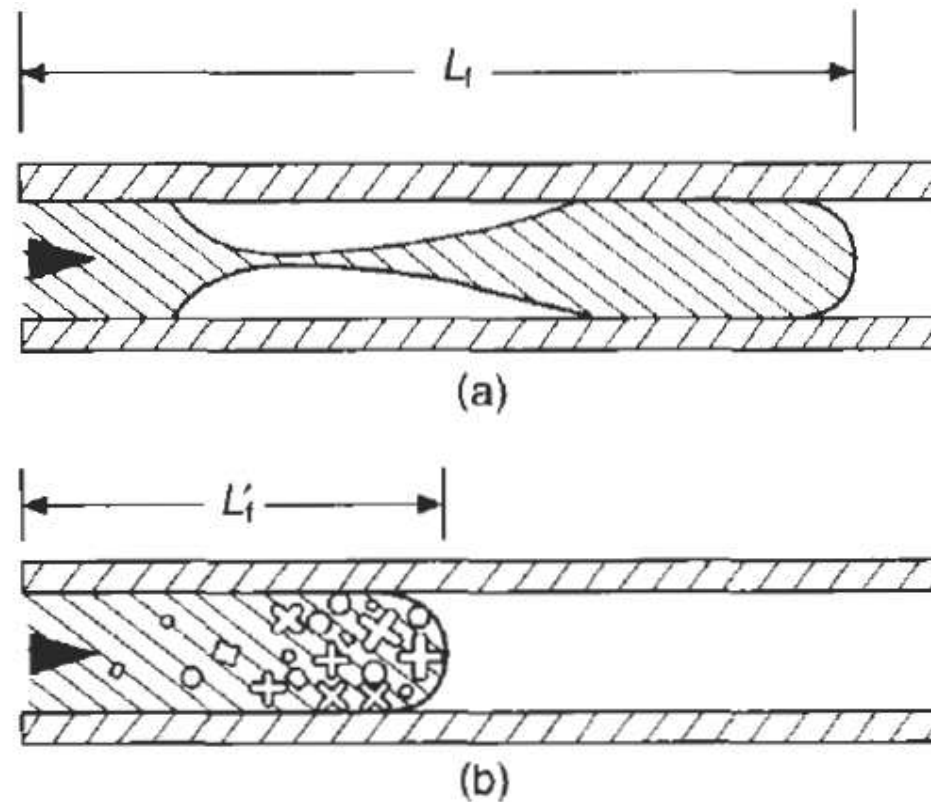
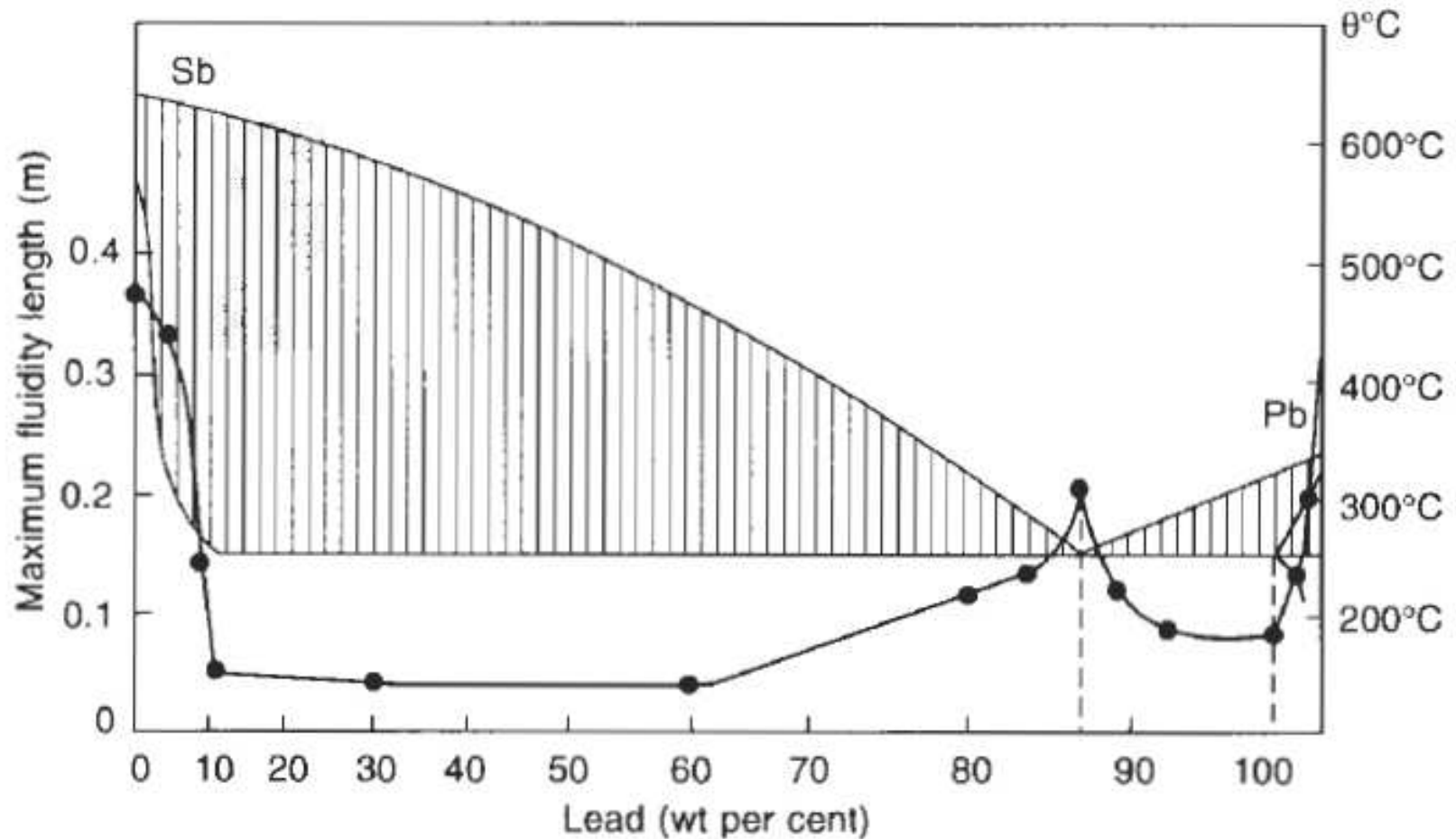
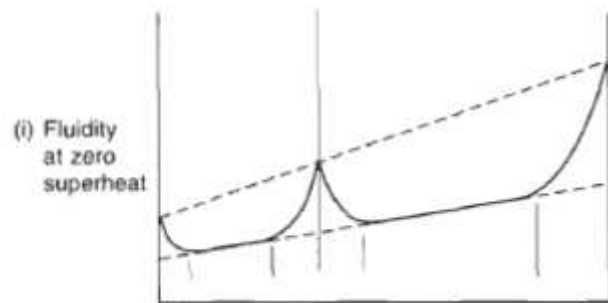
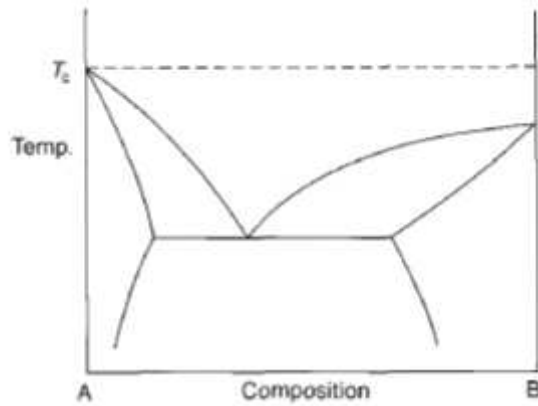


Figure 3.3 Flow arrest: (a) in pure metals by complete solidification; and (b) in long-freezing-range alloys by partial solidification.

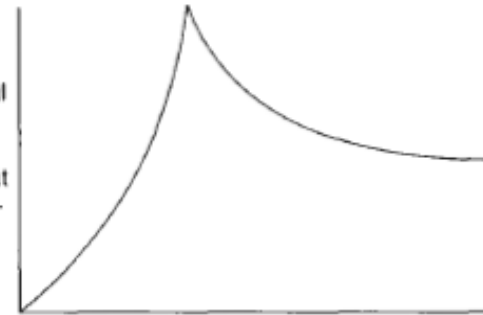
Fluidez de acordo com o intervalo de solidificação



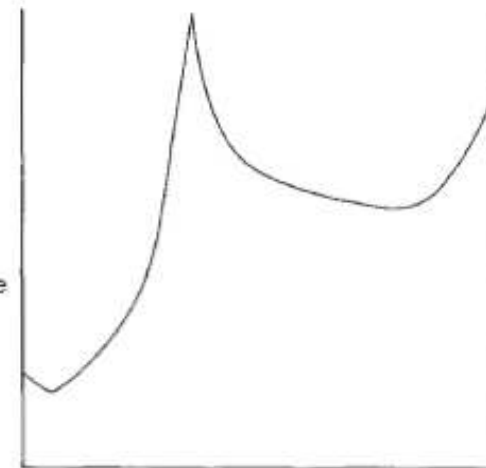
Influência do super-aquecimento



(ii) Additional fluidity due to superheat at temperature T_c



Total fluidity ((i) + (ii)) at casting temperature T_c



Efeito de um avanço turbulento na superfície do metal líquido

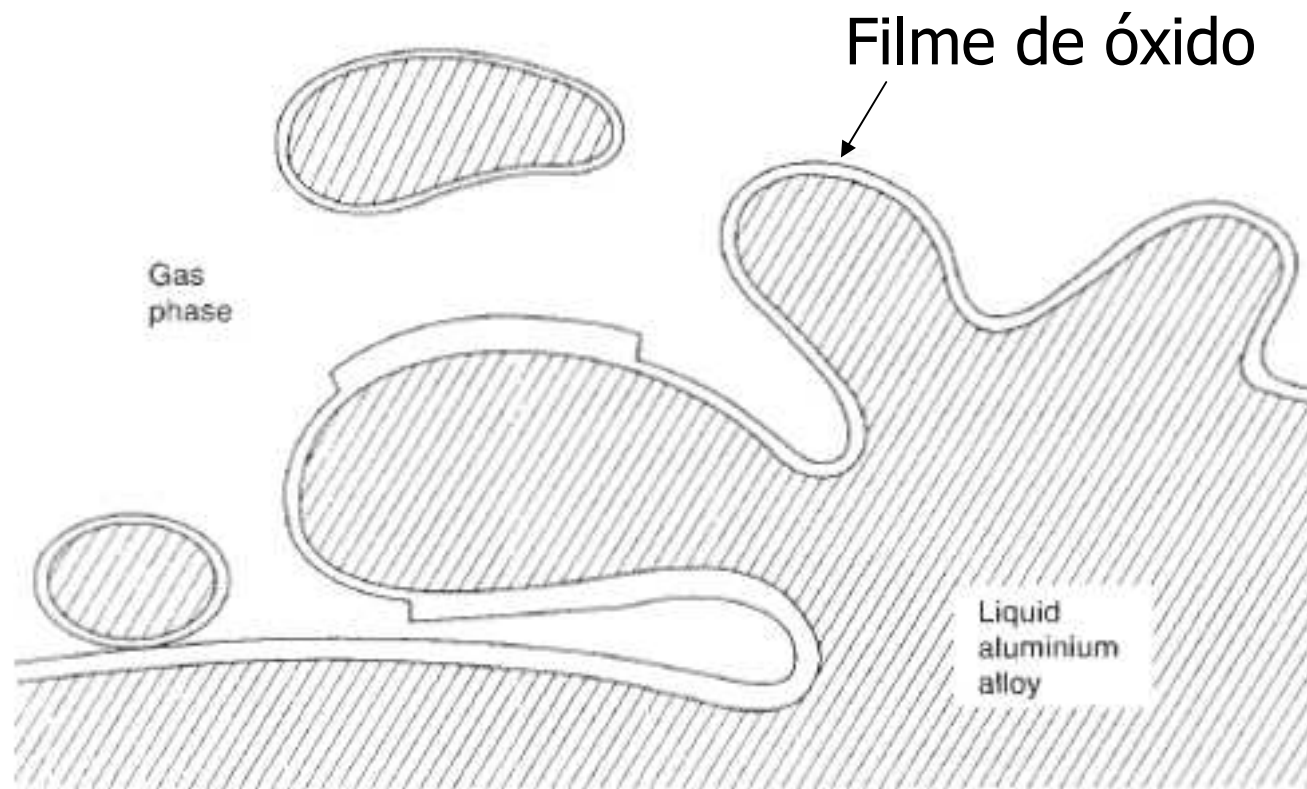


Figure 2.1 Sketch of a surface entrainment event.

Efeitos de alimentação intermitente

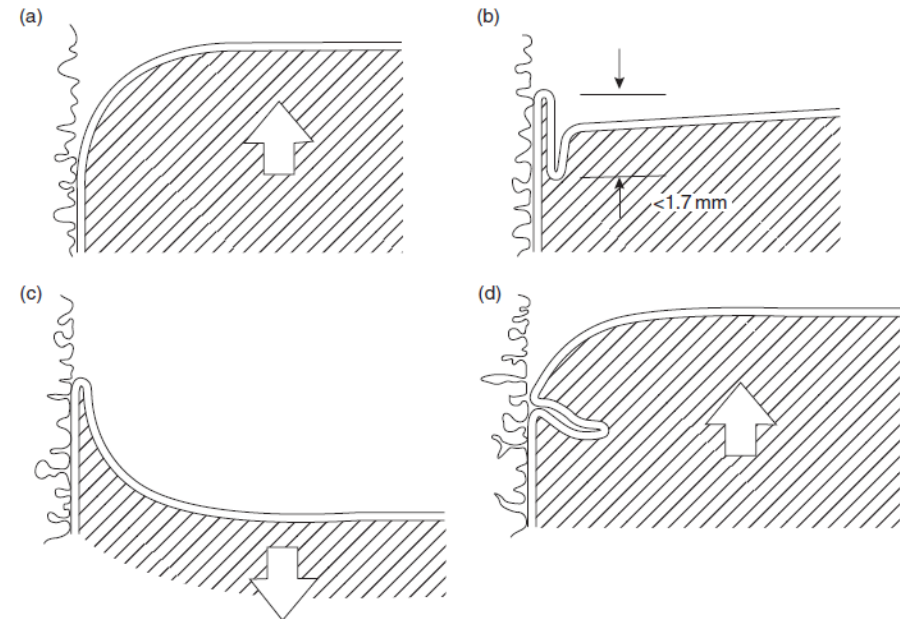
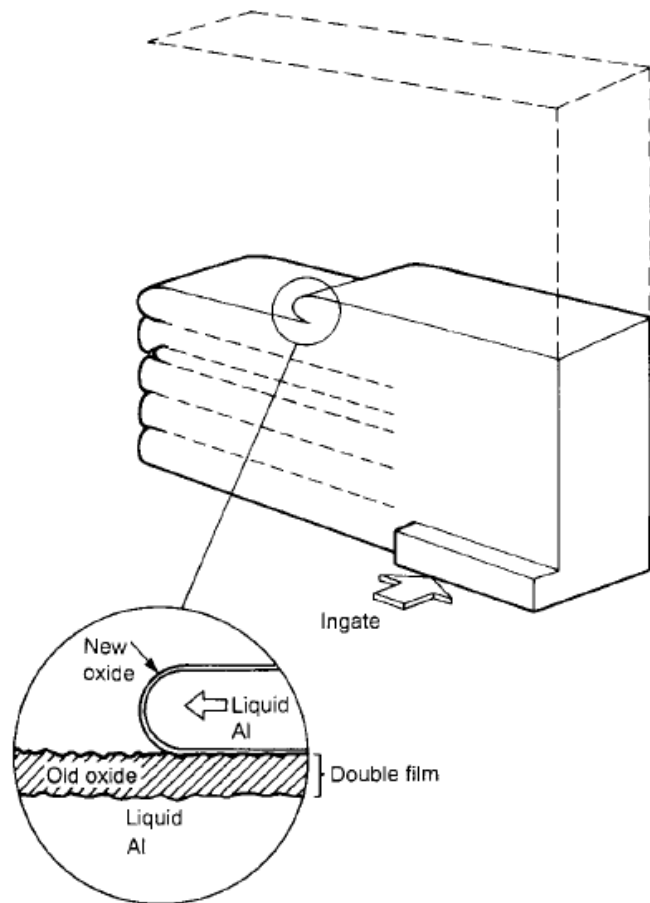
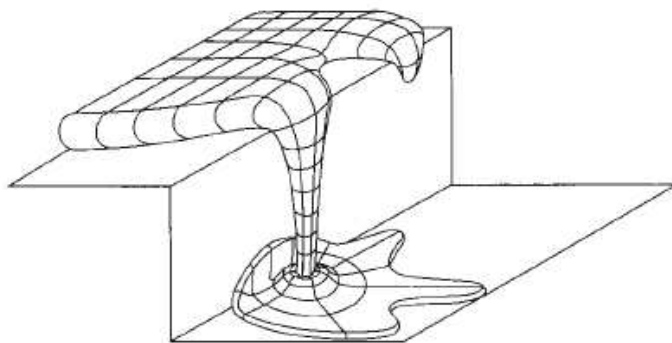


Figure 3.6 The creation of a bifilm crack by the reversal of the front, causing the meniscus to flatten and enfold in the excess surface area. Surface cracks of the order of a millimetre depth can be formed in this way.

Efeito "cascata" e projeção de metal líquido

Oxide flow tube defect from a fall



Projeção

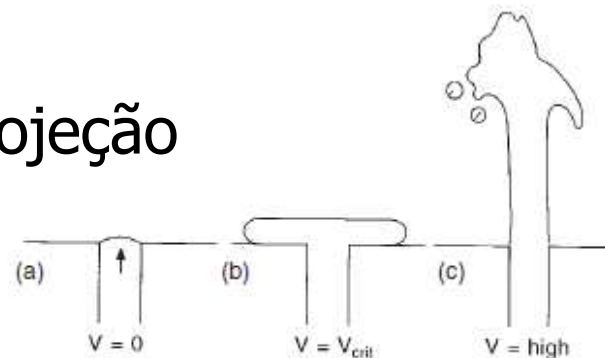
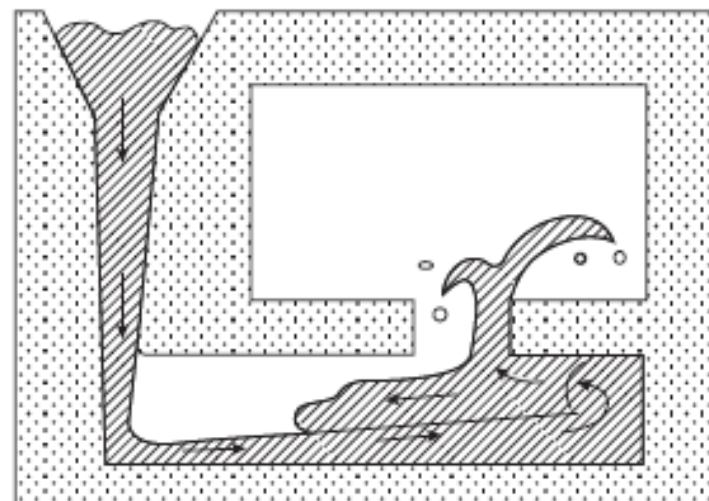
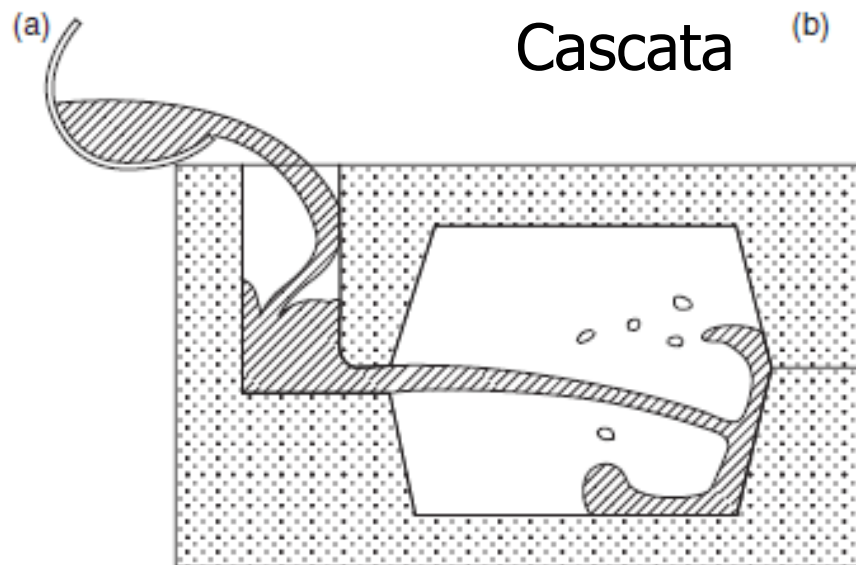
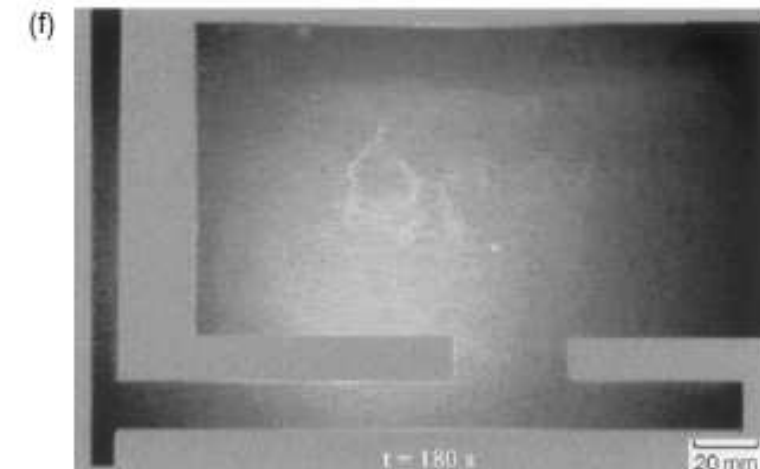
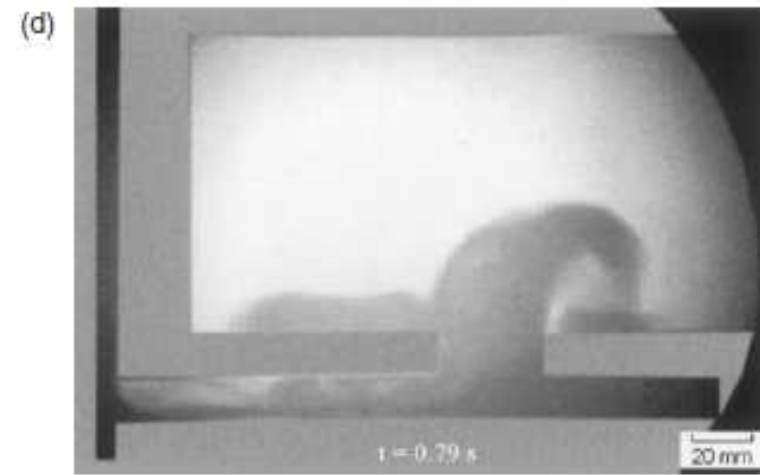
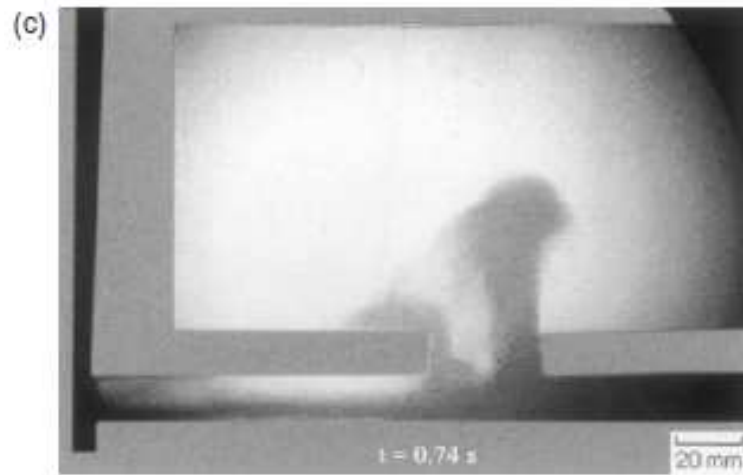


Figure 2.1 The extremes of velocity entering the mould from the gate; zero, critical and high.

$V_{crit} \approx 0,5 \text{ m/s}$ p/ a maioria dos metais



Efeito da projeção de metal líquido



Efeito de mudanças bruscas de área durante o preenchimento

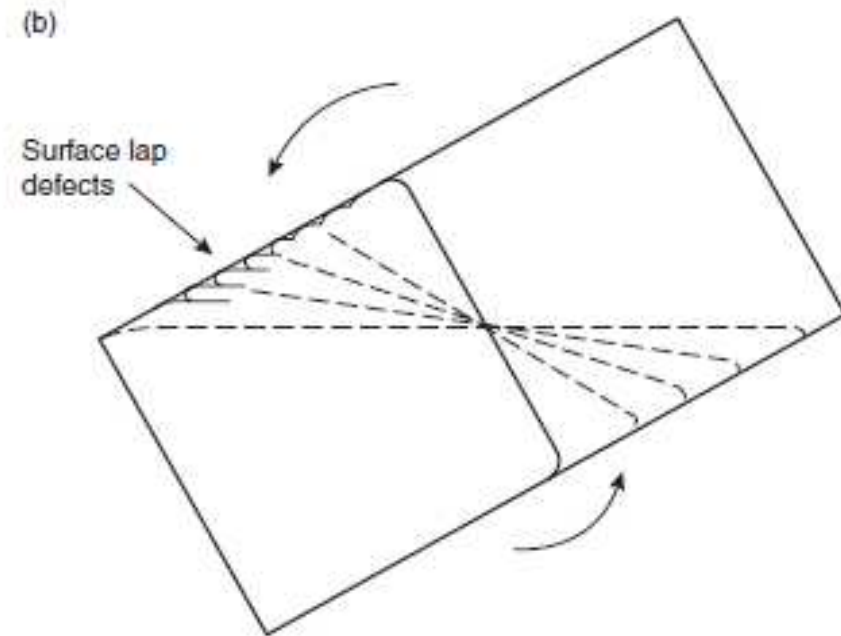
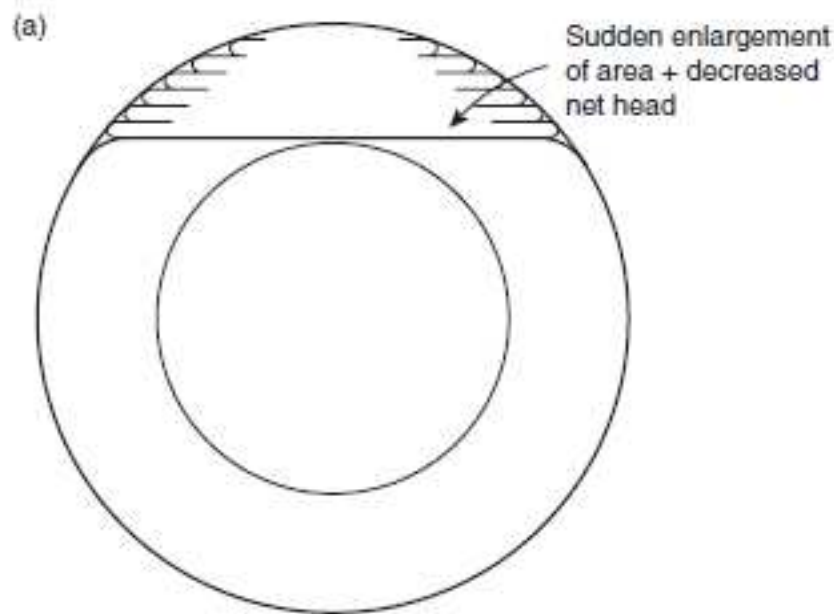


Figure 2.60 Common lap problems at low rates of rise of liquid surface in the mould (a) in a horizontal pipe or cylinder; (b) on the cope surface of a tilt casting.

Efeito de mudanças bruscas de área durante o preenchimento

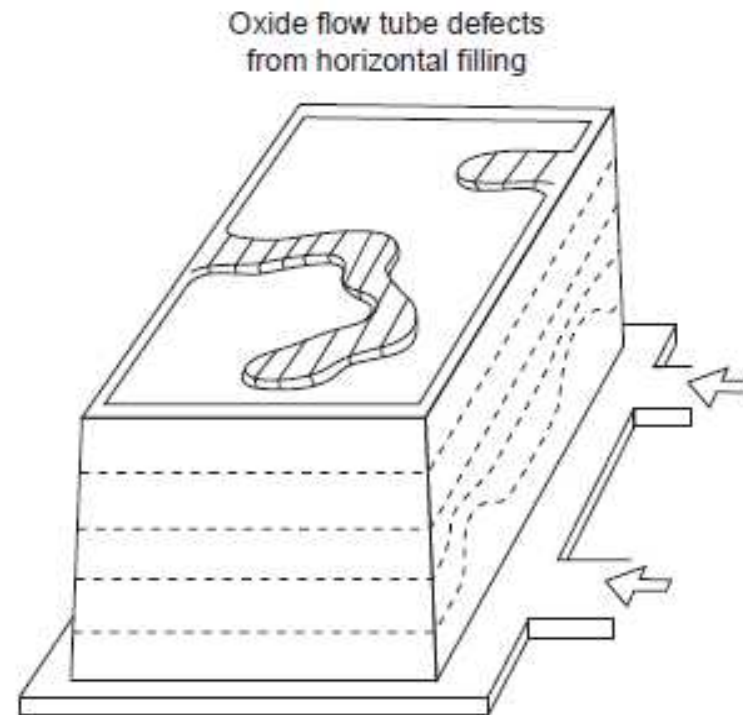


Figure 3.4 *The filling of a rectangular box type casting, illustrating the progressive advance of the front that characterizes the filling of vertical walls. The horizontal top, however, fills unpredictable meanders of river-like flows, leading to horizontal oxide flow tubes.*

Inclusão de bolhas devido a sistema de alimentação incorreto

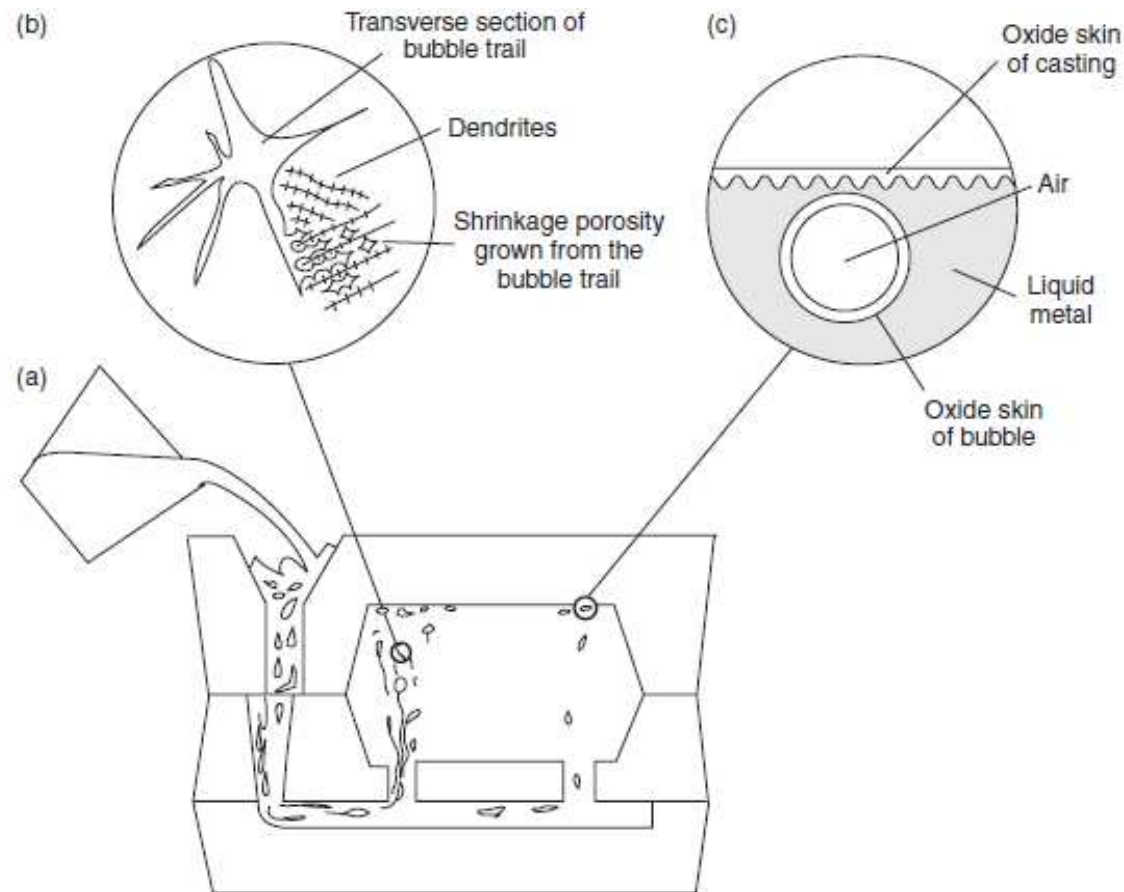
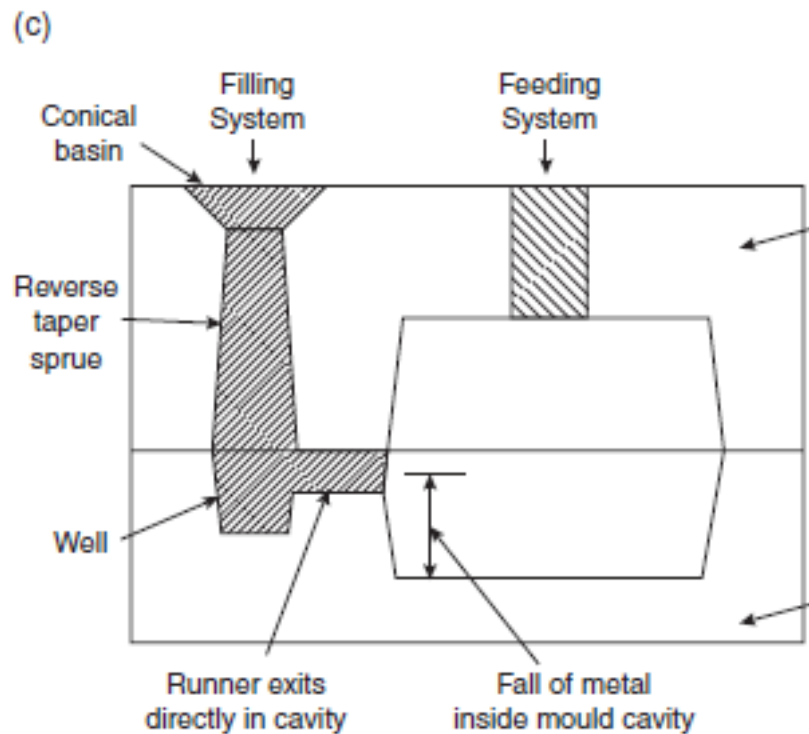
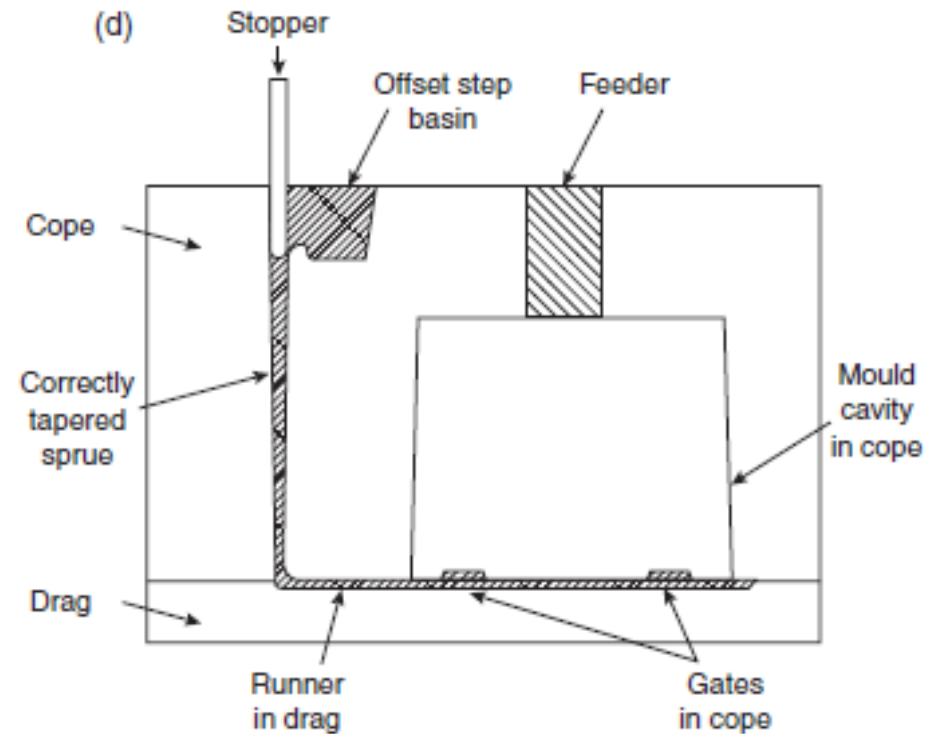


Figure 4.1 (a) Pattern of bubble damage in a casting; (b) trails invisible in radiography are usually visible on transverse sections; (c) small entrained air bubbles do not have sufficient buoyancy to break the double oxide barrier to escape to the atmosphere.

Exemplo

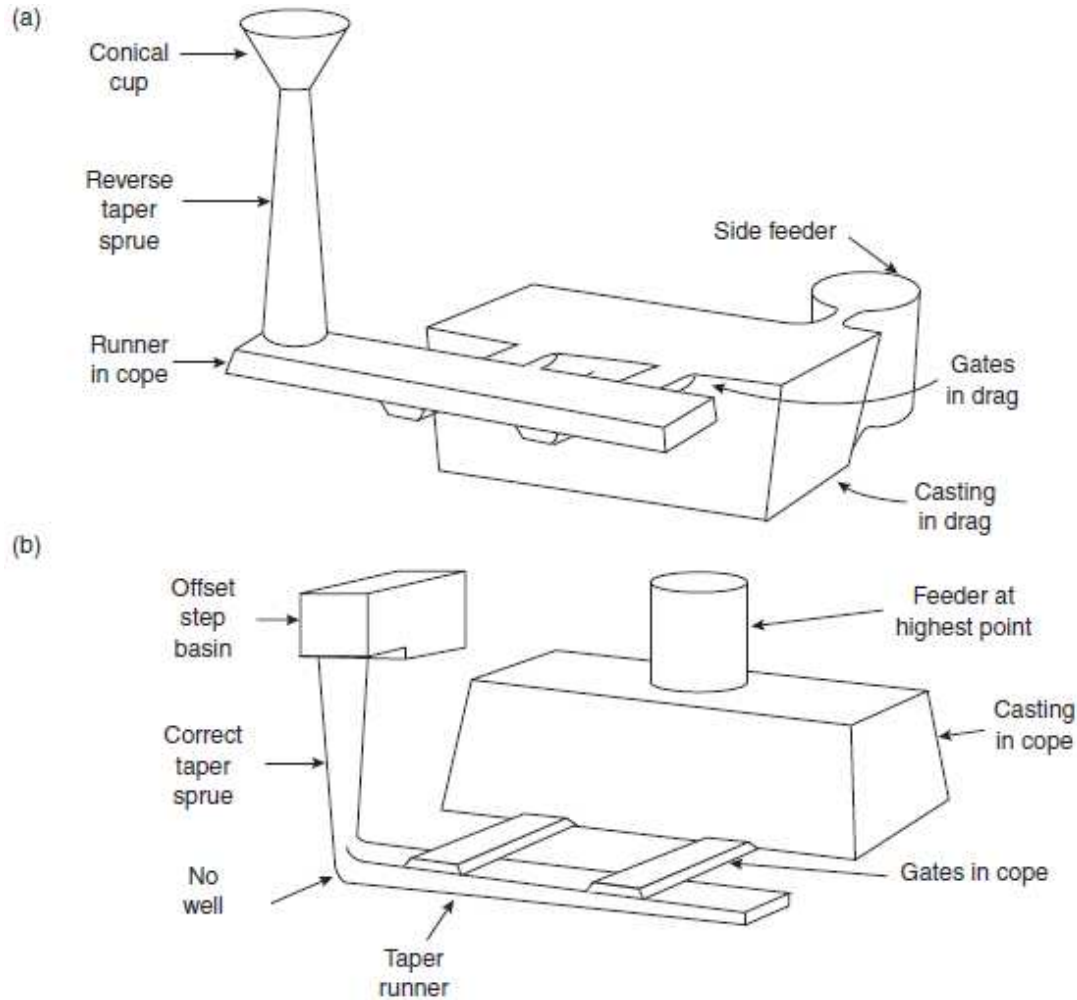


Ruim



Bom

Exemplo



Ruim

Bom

Bacia de vazamento

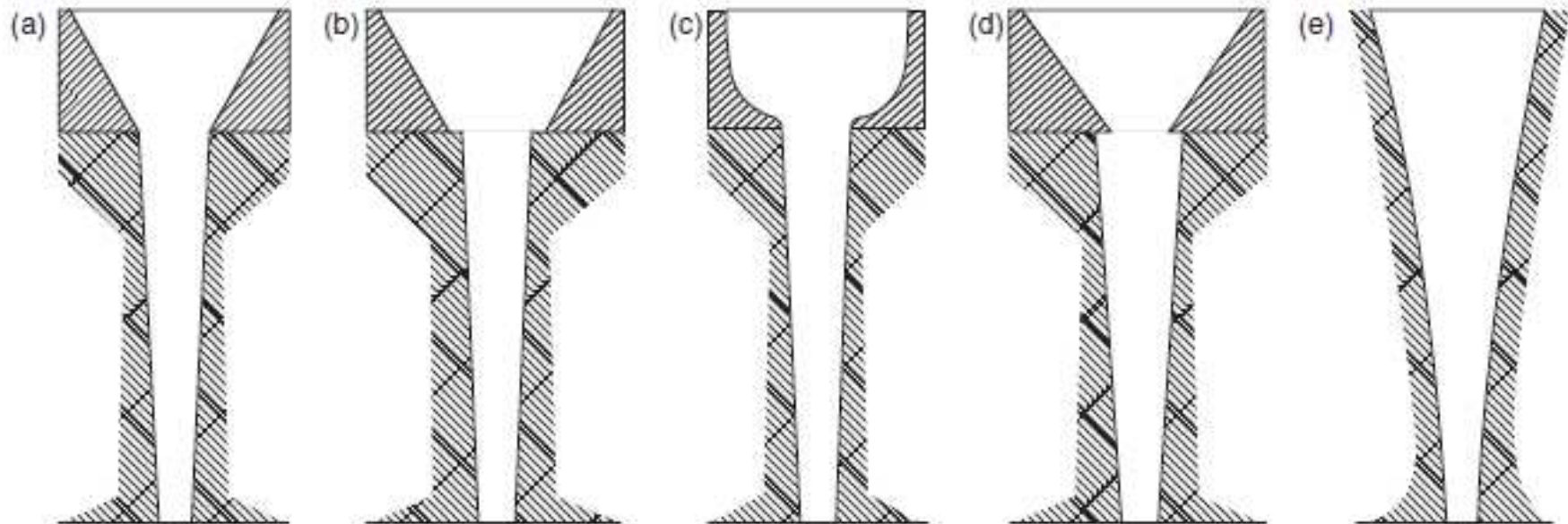


Figure 2.8 A rogues gallery of non-recommended scrap generating systems. Conical basin and sprue combinations showing (a) perhaps least damaging; (b) basin too large; (c) cup form; (d) basin too small; (e) enlarged sprue to act as a combined basin and sprue.

TODOS OS CASOS ACIMA NÃO SÃO RECOMENDADOS

Bacia de vazamento

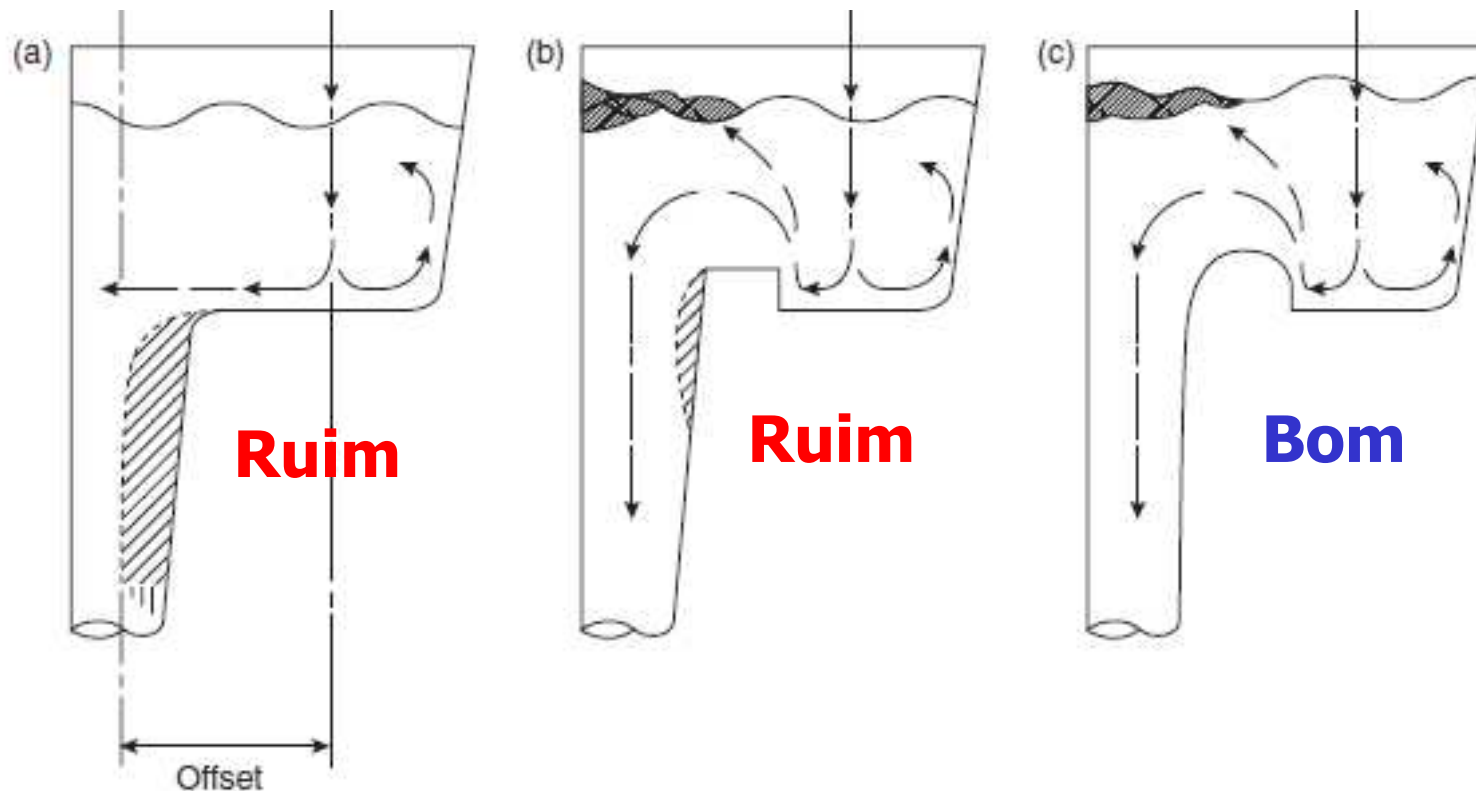


Figure 2.9 Offset pouring basins (a) without step (definitely not recommended); (b) sharp step (not recommended); (c) radiused step (recommended).

Bacia de vazamento

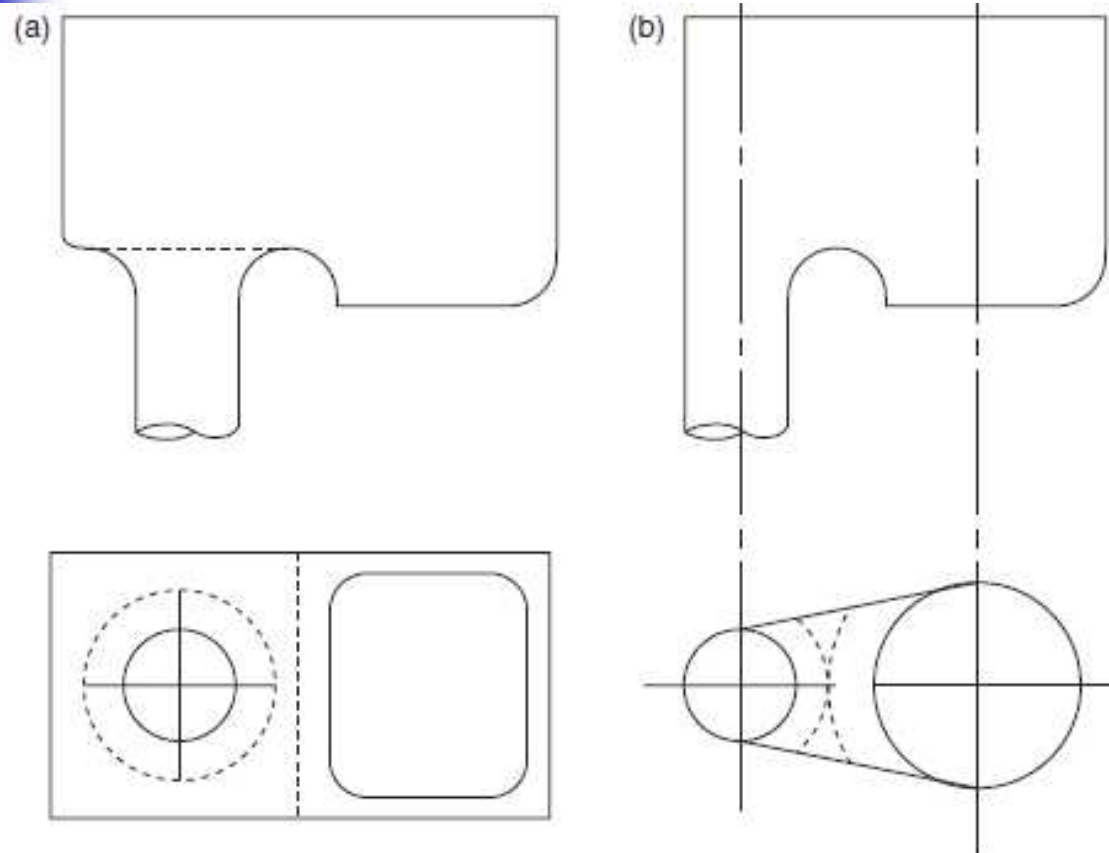


Figure 2.11 Side and plan views of offset basins (a) conventional rectangular; (b) slimmed shape to streamline flow and improve metal yield.

Melhor

Canal de descida

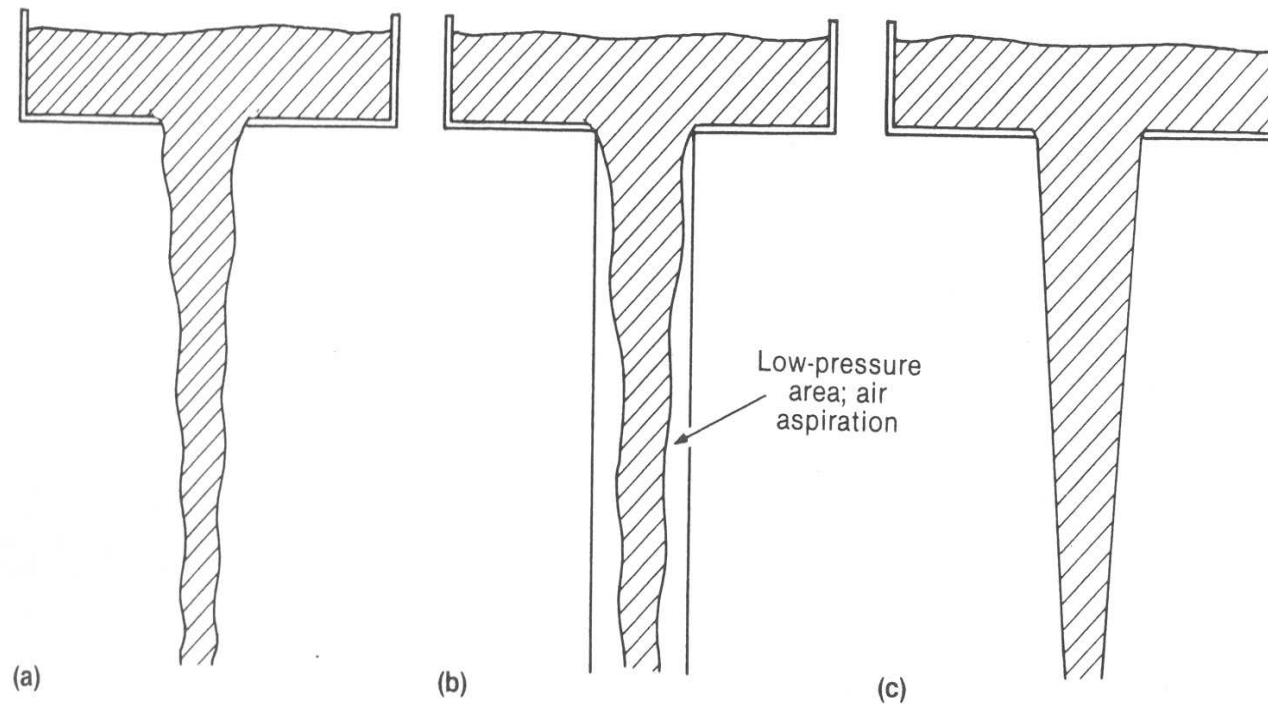


Fig. 3 Schematic showing the advantages of a tapered sprue over a straight-sided sprue. (a) Natural flow of a free-falling liquid. (b) Air aspiration induced by liquid flow in a straight-sided sprue. (c) Liquid flow in a tapered sprue

Canal de descida

$$\frac{A_1}{A_2} = \sqrt{\frac{H_2}{H_1}}$$

$$t = \frac{V}{A_2 \cdot C \cdot \sqrt{2gH_2}}$$

t – tempo de preenchimento estimado (alimentação por baixo)

V – volume de metal

C – eficiência do canal (C=1 p/ atrito zero)

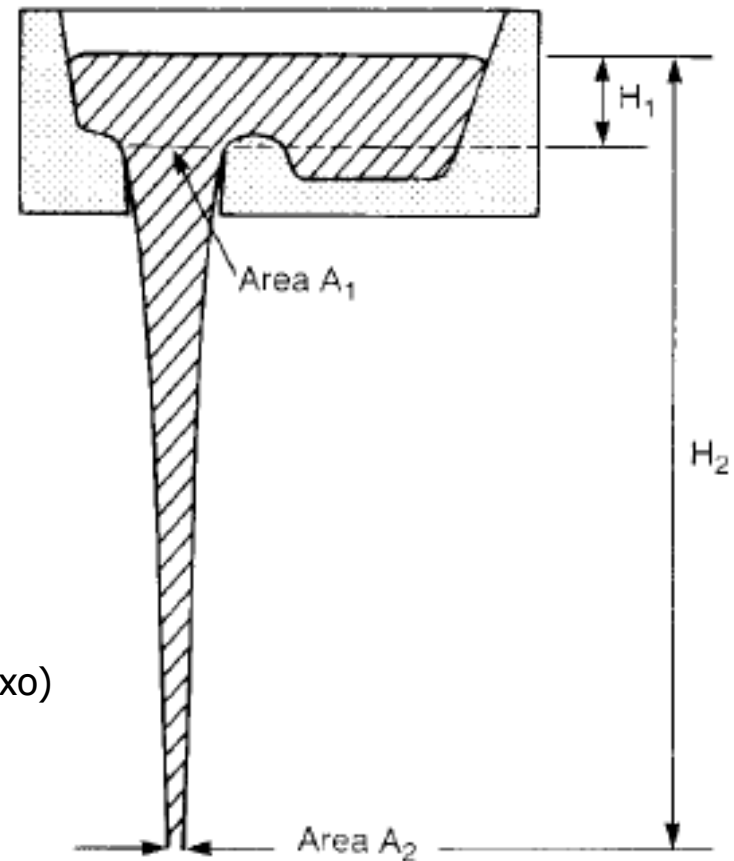


Figure 2.13 *The geometry of the stream falling freely from a basin.*

O canal de descida e a curva do filete de metal líquido

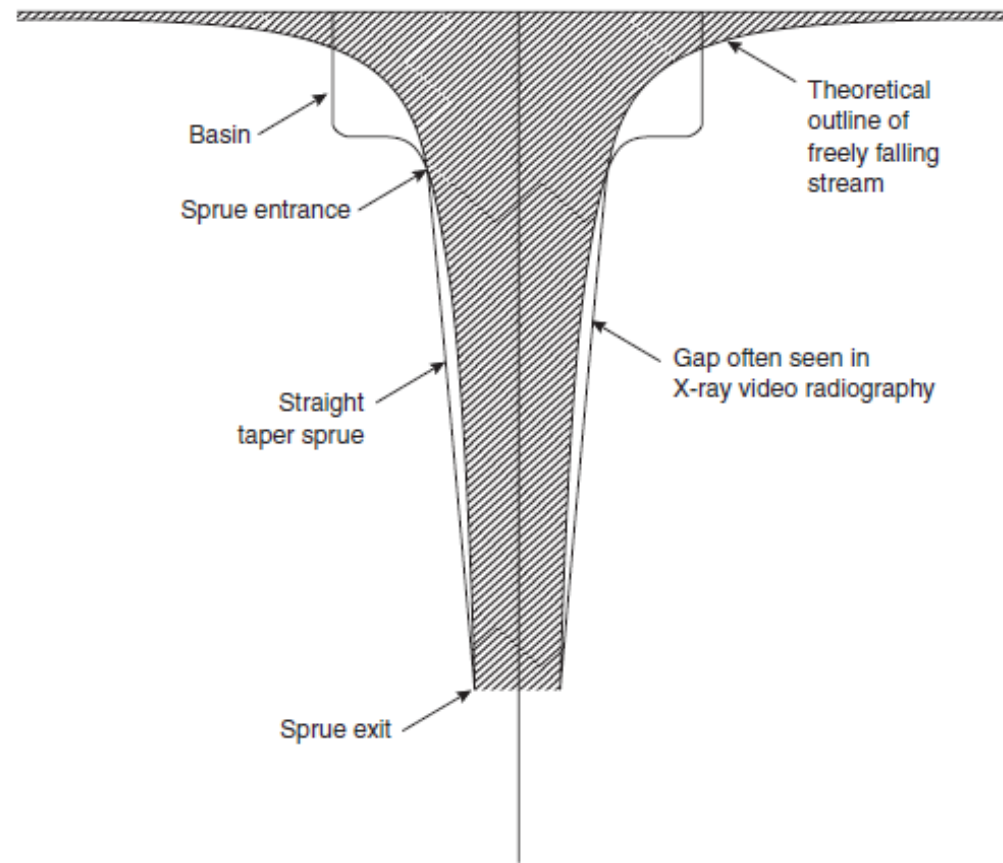
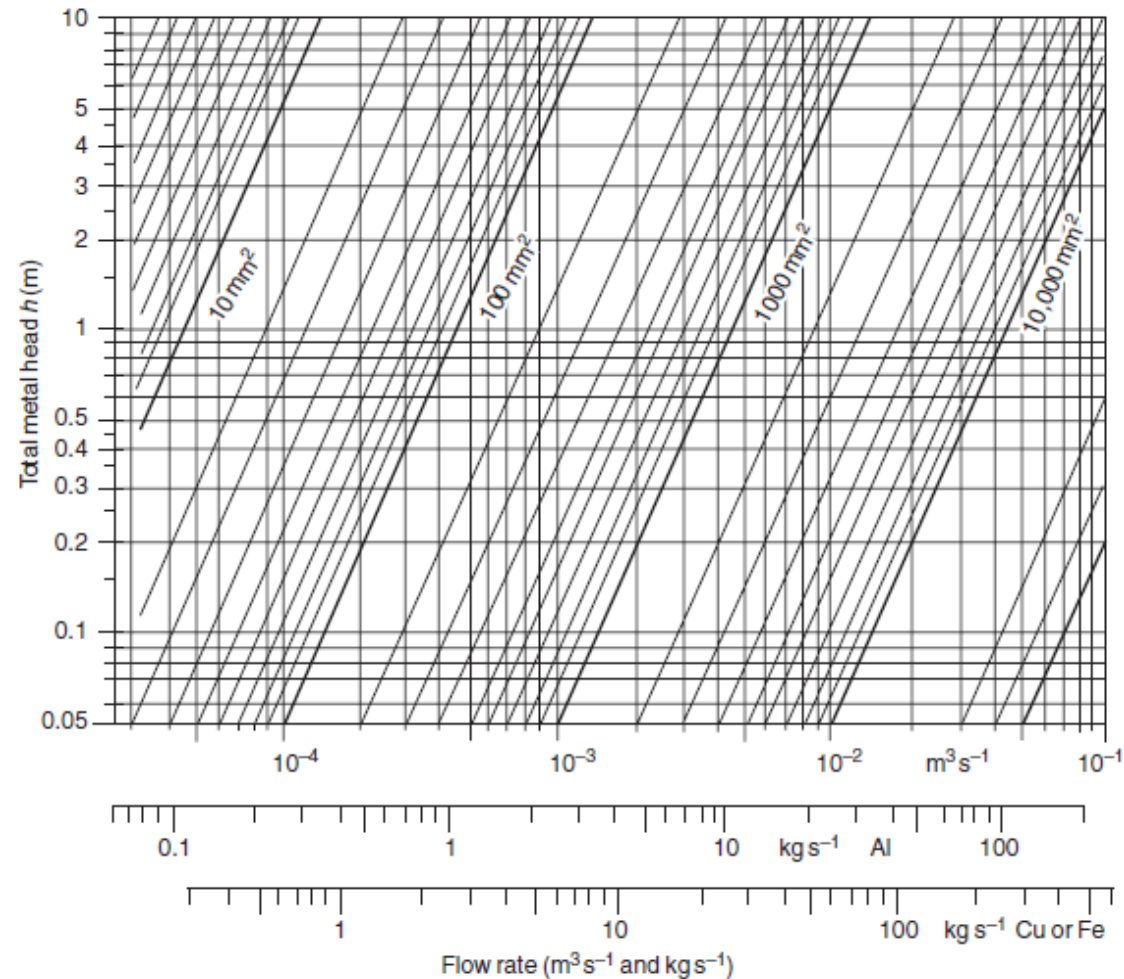


Figure 2.15 The theoretical hyperbola shape of the falling stream, illustrating the complicating effects of the basin and sprue entrance.

Diagrama de áreas para canais de descida

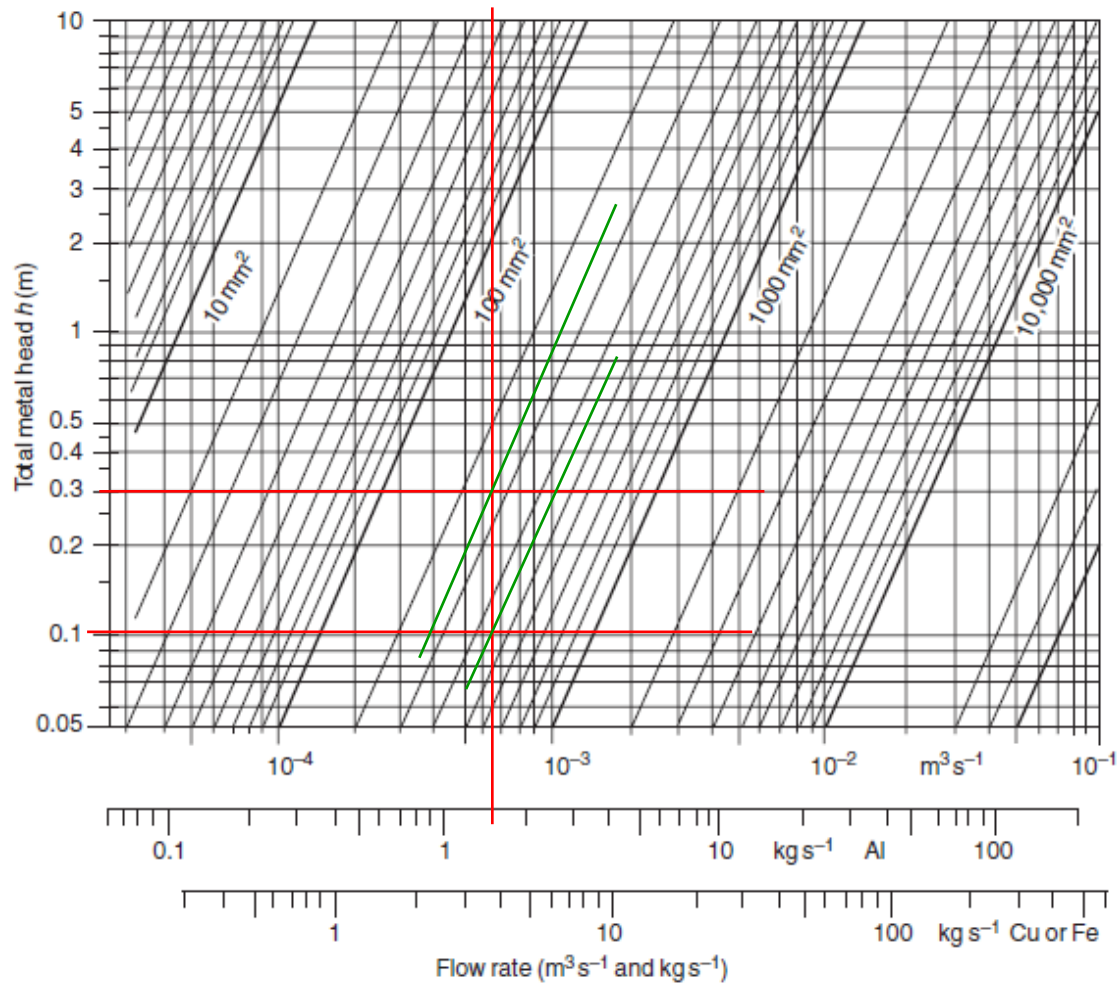




Exemplo de uso

- Liga de Al
- Taxa de alimentação média: 1,0 Kg/s
- Usar taxa inicial 1,5x maior: 1,5 Kg/s
- $H1 = 100 \text{ mm}$
- $H2 = 300 \text{ mm}$

Exemplo de uso



$A1 \approx 450 mm^2$
 $A2 \approx 250 mm^2$

Usar 1,2.A1
para compensar
erro da geometria

Portanto:
 $A1 \approx 540 mm^2$

Base do canal de descida

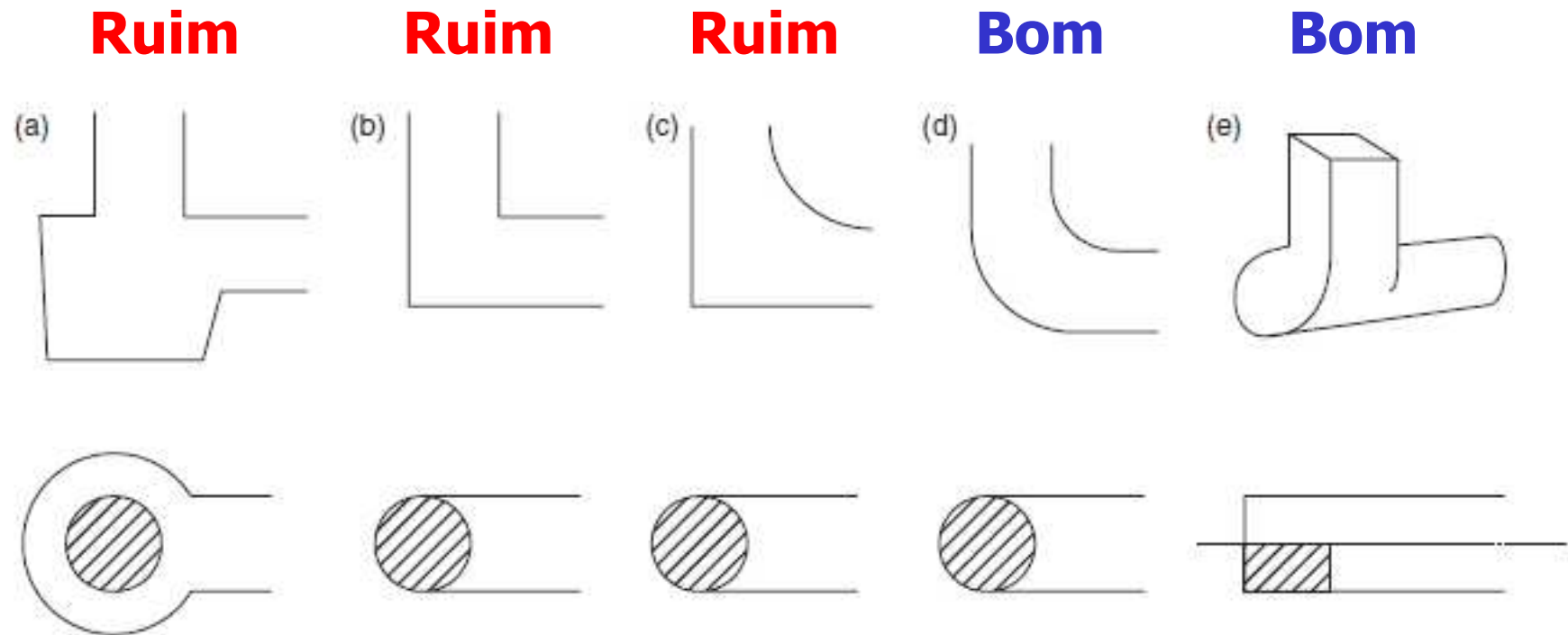


Figure 2.19 A variety of spruelrunner junctions in side and plan views from poorest (a) to best (d). The offset junction at (e) forms a vortex flow along the cylindrical runner.

Base do canal de descida

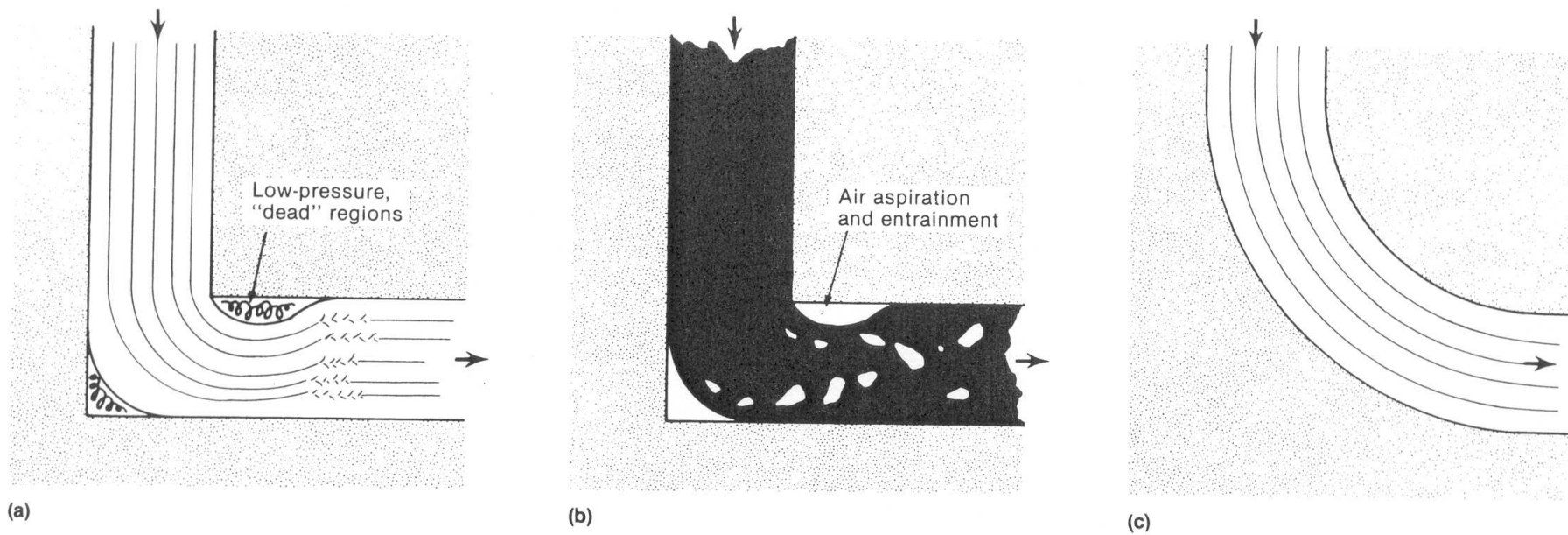
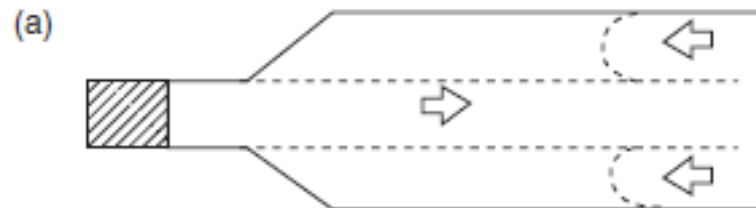


Fig. 7 Schematic illustrating fluid flow around right-angle and curved bends in a gating system. (a) Turbulence resulting from a sharp corner. (b) Metal damage resulting from a sharp corner. (c) Streamlined corner that minimizes turbulence and metal damage

Base do canal de descida

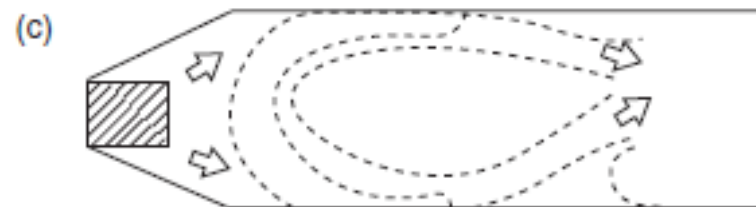
Ruim



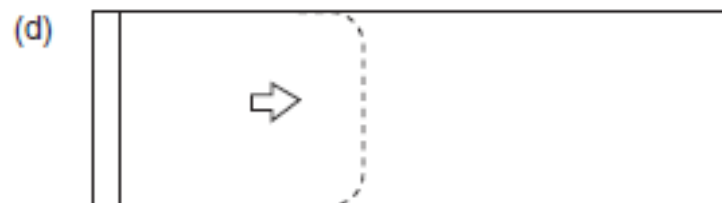
Ruim



Ruim



Bom



Canais de distribuição

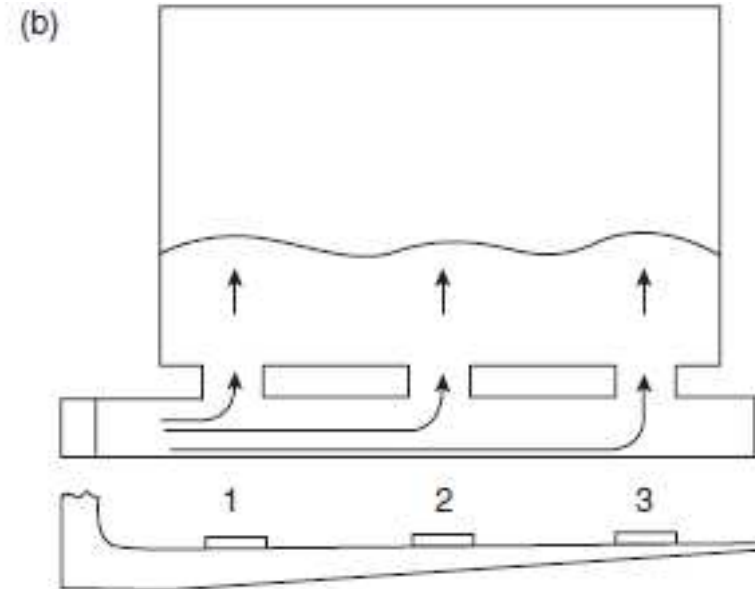
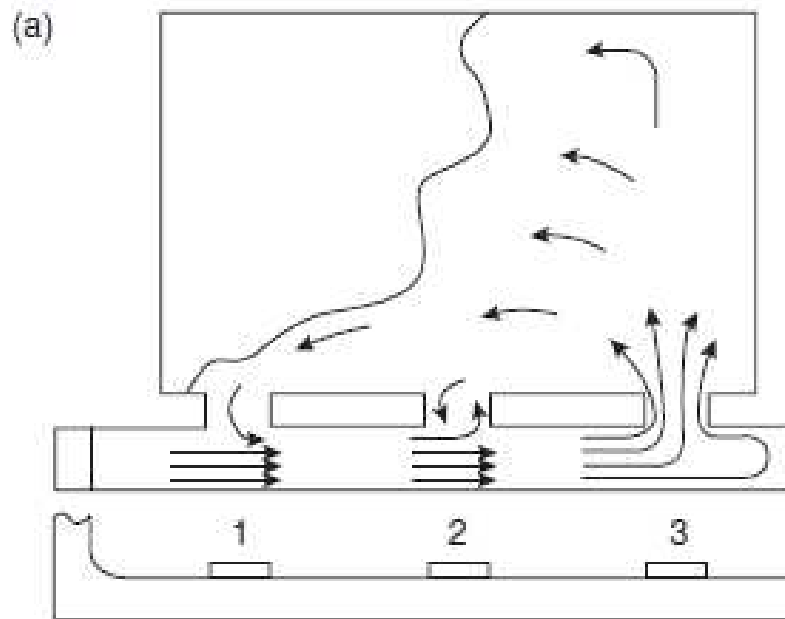


Figure 2.26 (a) An unbalanced delivery of melt into the mould as a result of an incorrect runner design; (b) a tolerably balanced system.

Uso de filtros

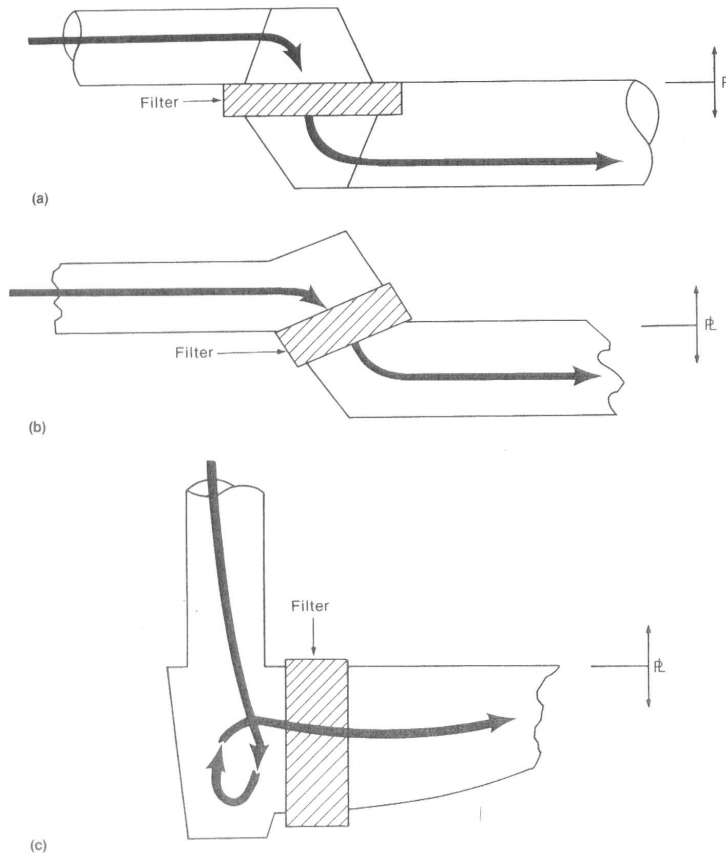


Fig. 16 Common methods of filter placement in horizontally parted molds. (a) Parallel to parting line. (b) Between 0 and 90° to parting line. (c) 90° to parting line. Arrows indicate the direction of metal flow.

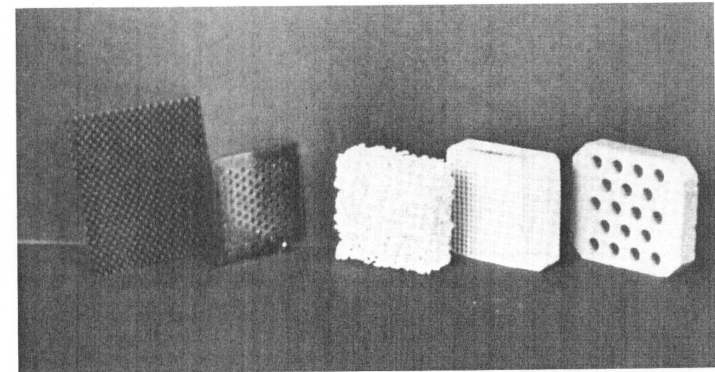


Fig. 14 Several common filtration and flow modification devices (from left to right): strainer core, extruded ceramic filter, ceramic foam filter, mica screen, and woven fabric screen. The two types of ceramic filters are by far the most widely used.

Canais de ataque

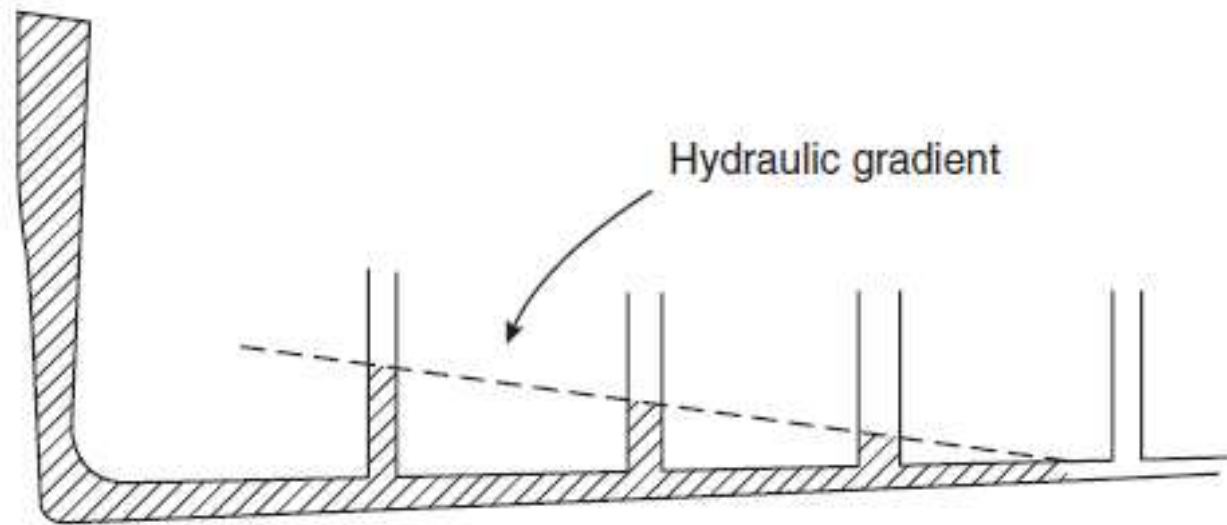


Figure 2.29 *The partial filling of vertical ingates along the length of a runner.*

Canais de ataque

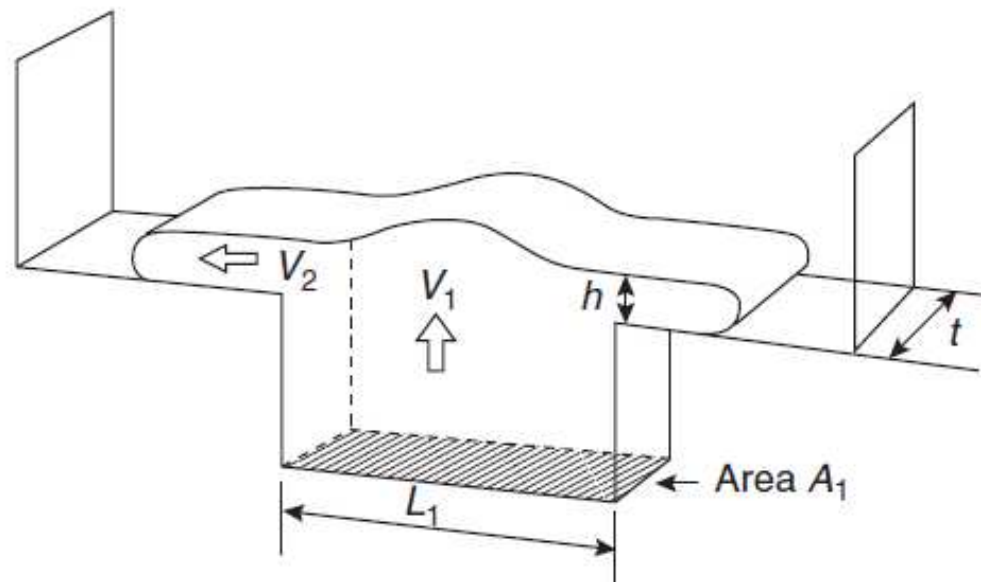


Figure 2.30 Sideways flow inside mould cavity.

$$L_1 \leq 2h$$

$$p/Alh = 13 \text{ mm}$$

p/ferrosos

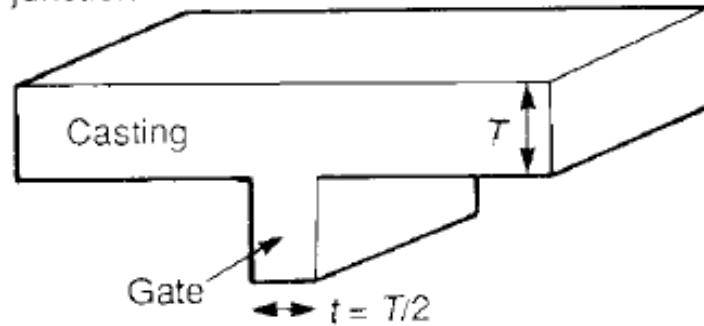
$$h = 10 \text{ mm}$$

Quando L_1 precisa ser maior então usar vários:

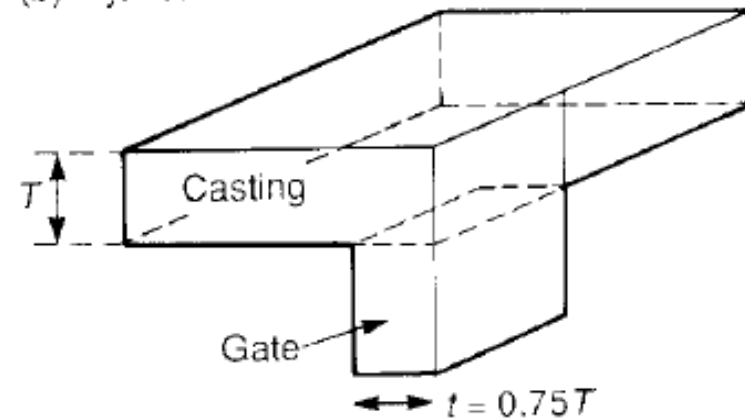
$$N \geq L_1/2h$$

Canais de ataque

(a) T-junction



(b) L-junction



(c) Casting extension

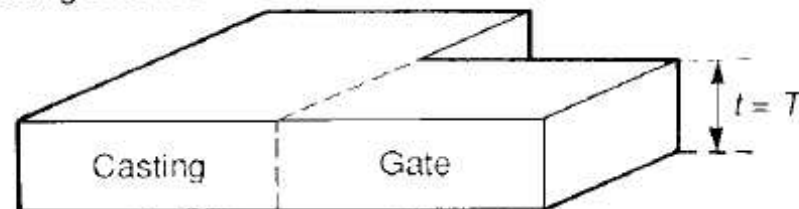
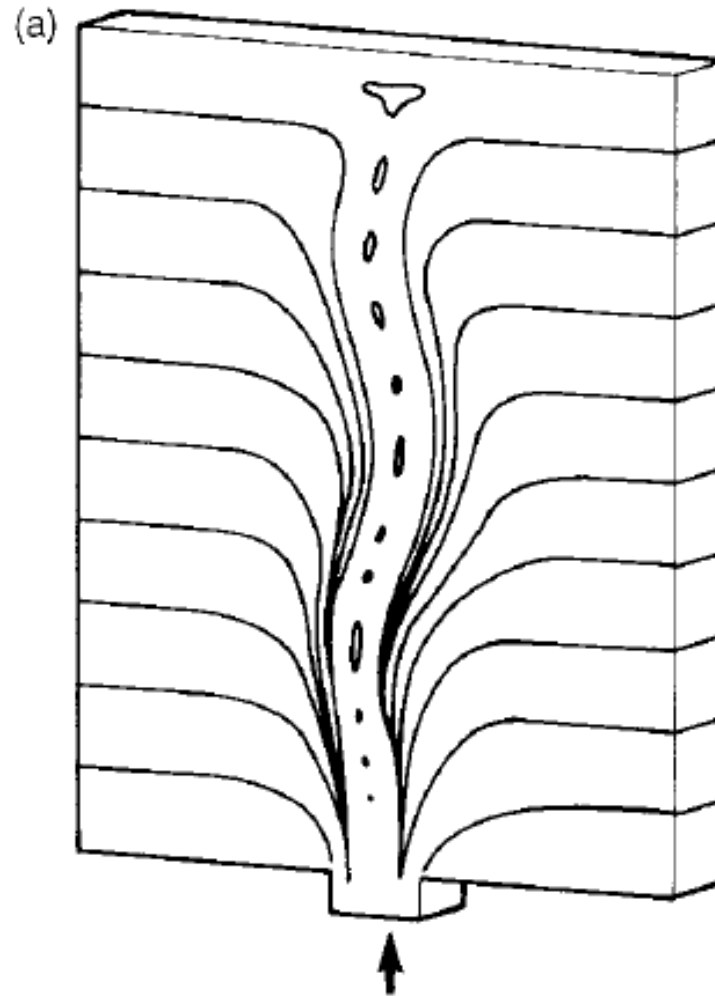


Figure 2.31 Maximum allowable gate thickness to avoid a hot spot at the junction with the casting.

Efeito do canal de ataque em placas



Alimentação indireta para placas

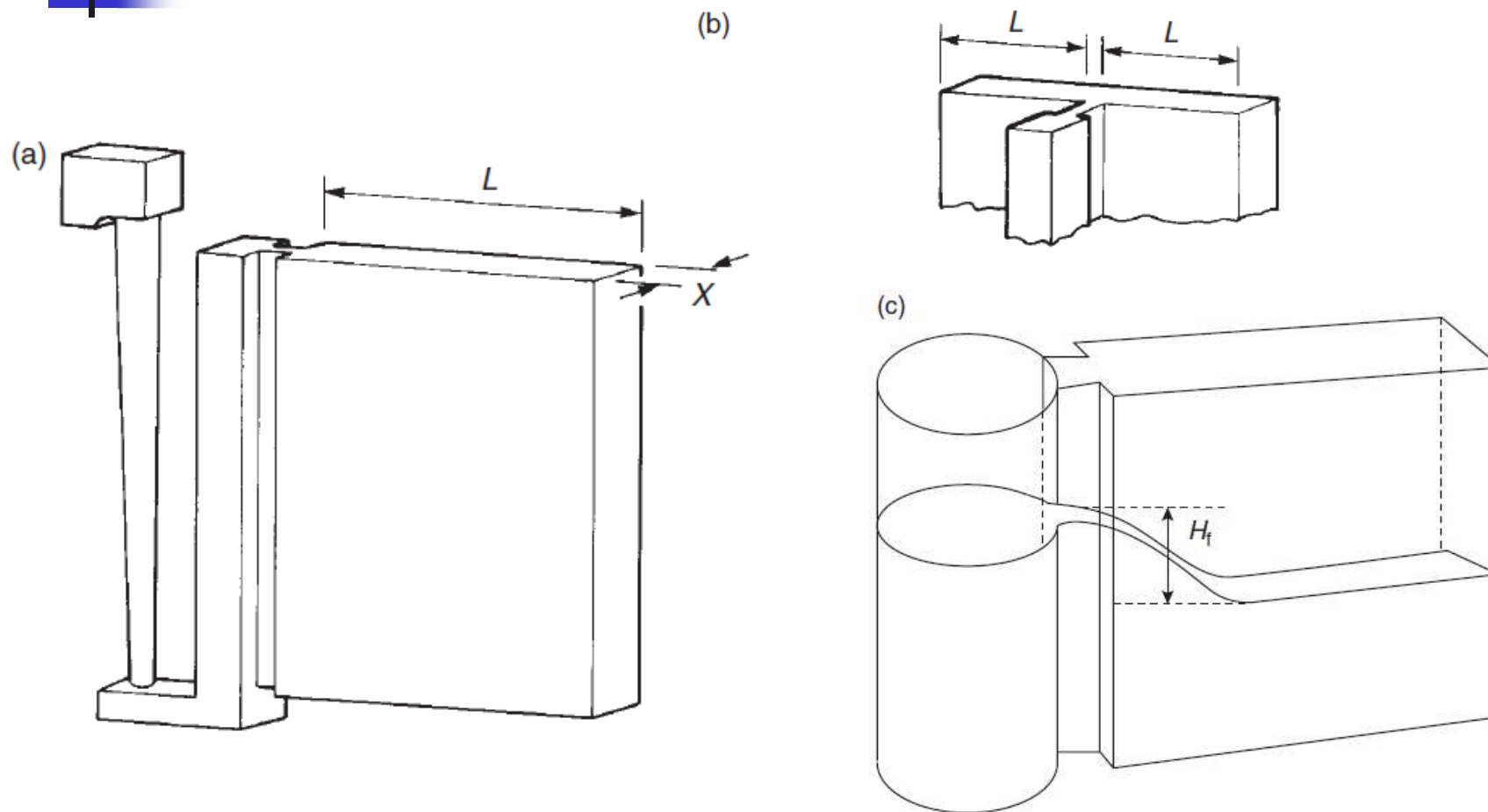


Figure 2.39 Riser and slot gate to both gate and feed a vertical plate from (a) its side, or (b) its centre.

Efeito de sopro do macho

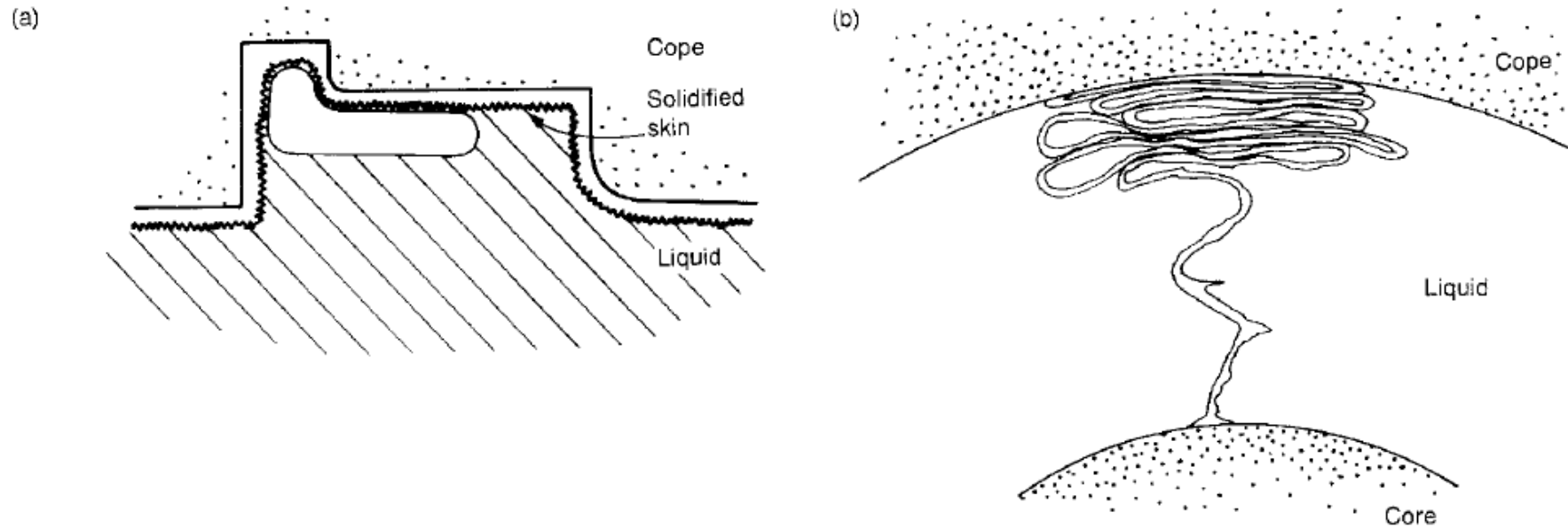


Figure 5.1 (a) A core blow—a trapped bubble containing core gases evolved after some solidification; (b) an exfoliated dross defect produced by copious gas from a core blow prior to solidification.

Prevenindo o sopro do macho

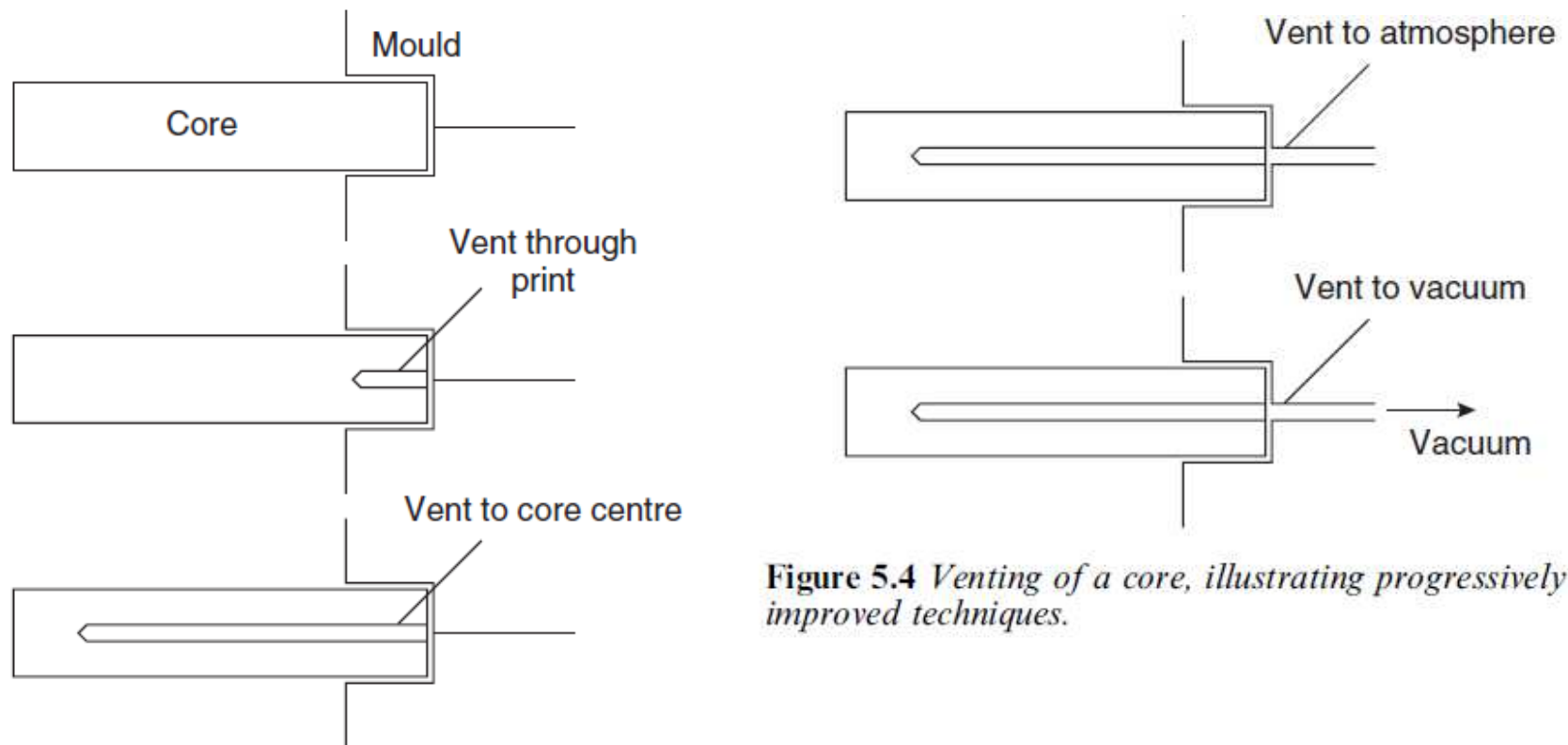


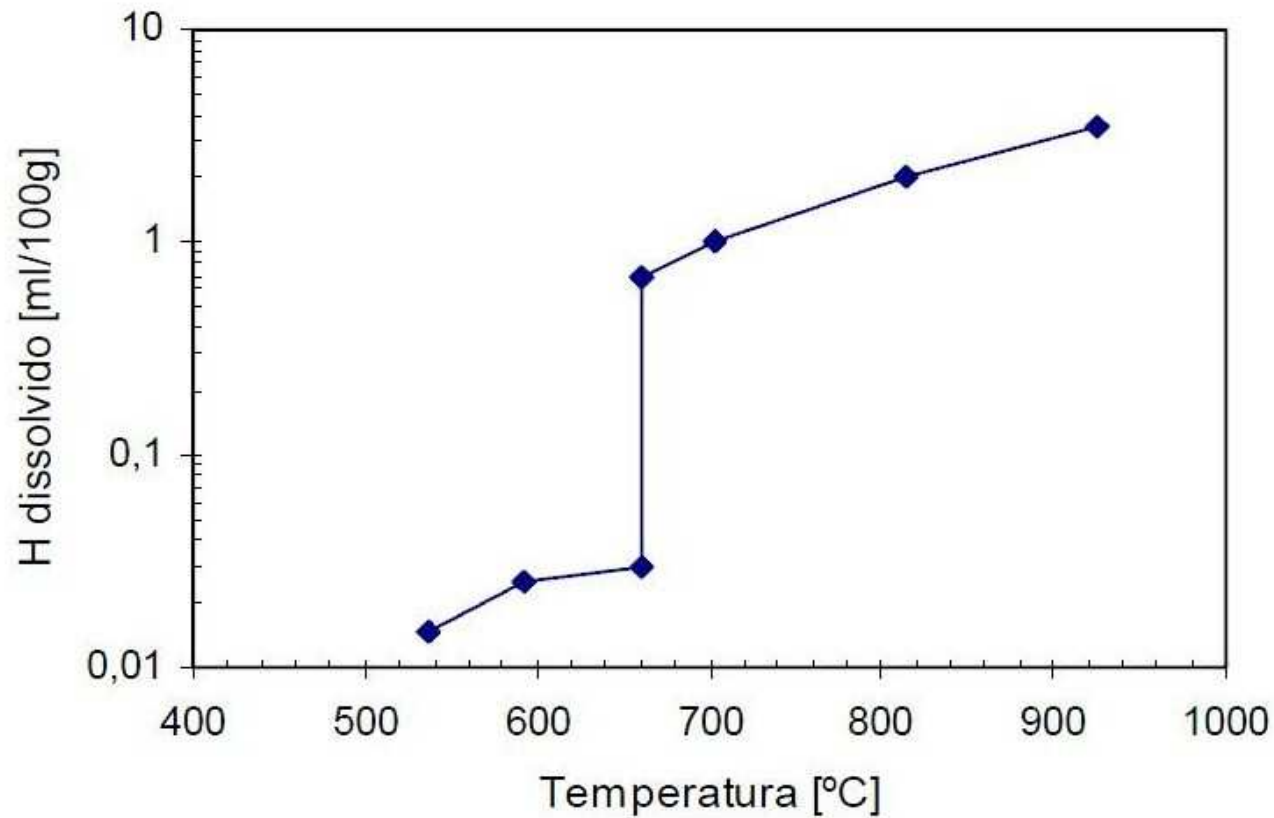
Figure 5.4 *Venting of a core, illustrating progressively improved techniques.*



Importante: Metal líquido de qualidade

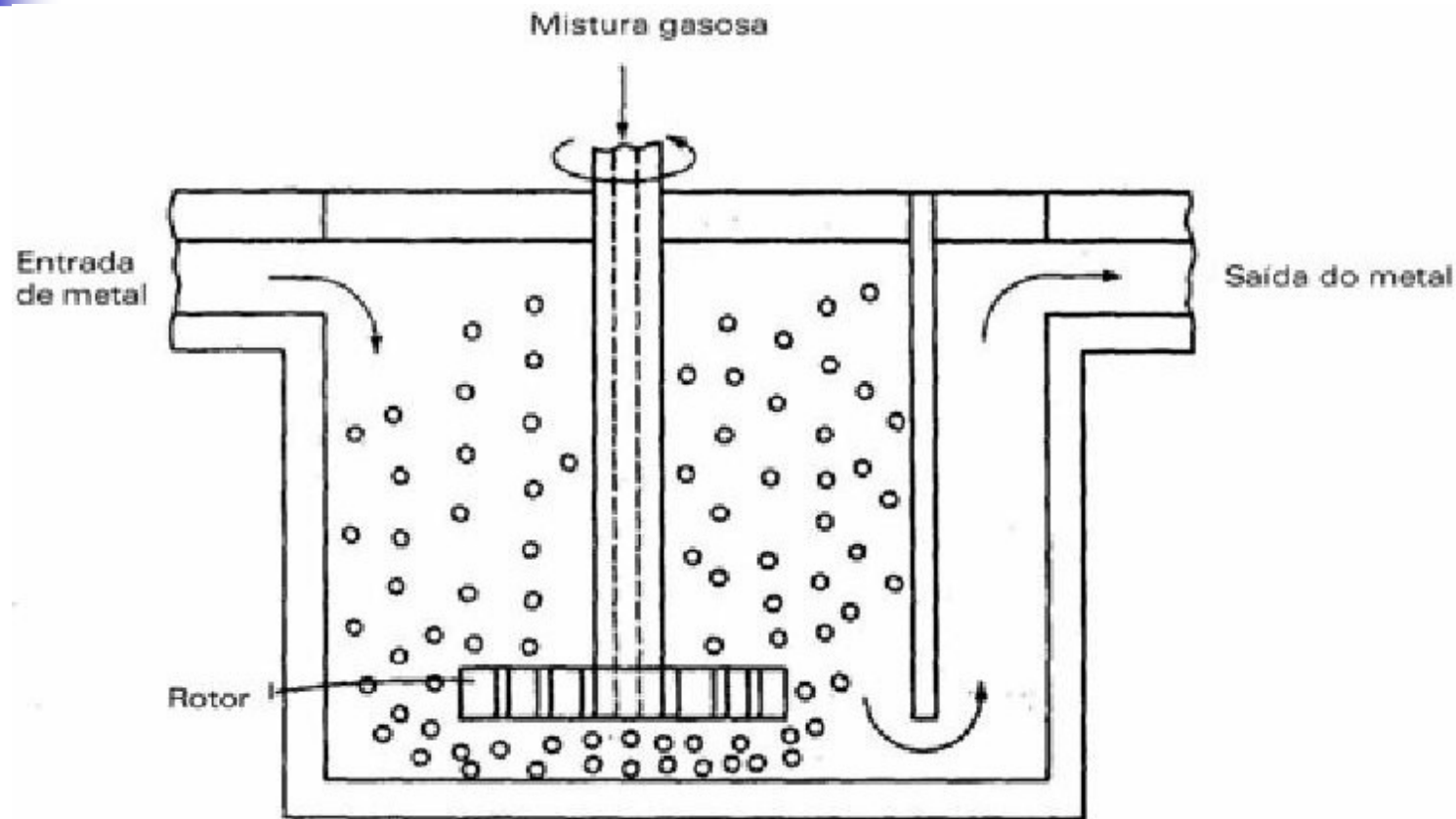
- Livre de gases
- Livre de inclusões de escória
- Na composição química correta

Exemplo: desgaseificação de Al



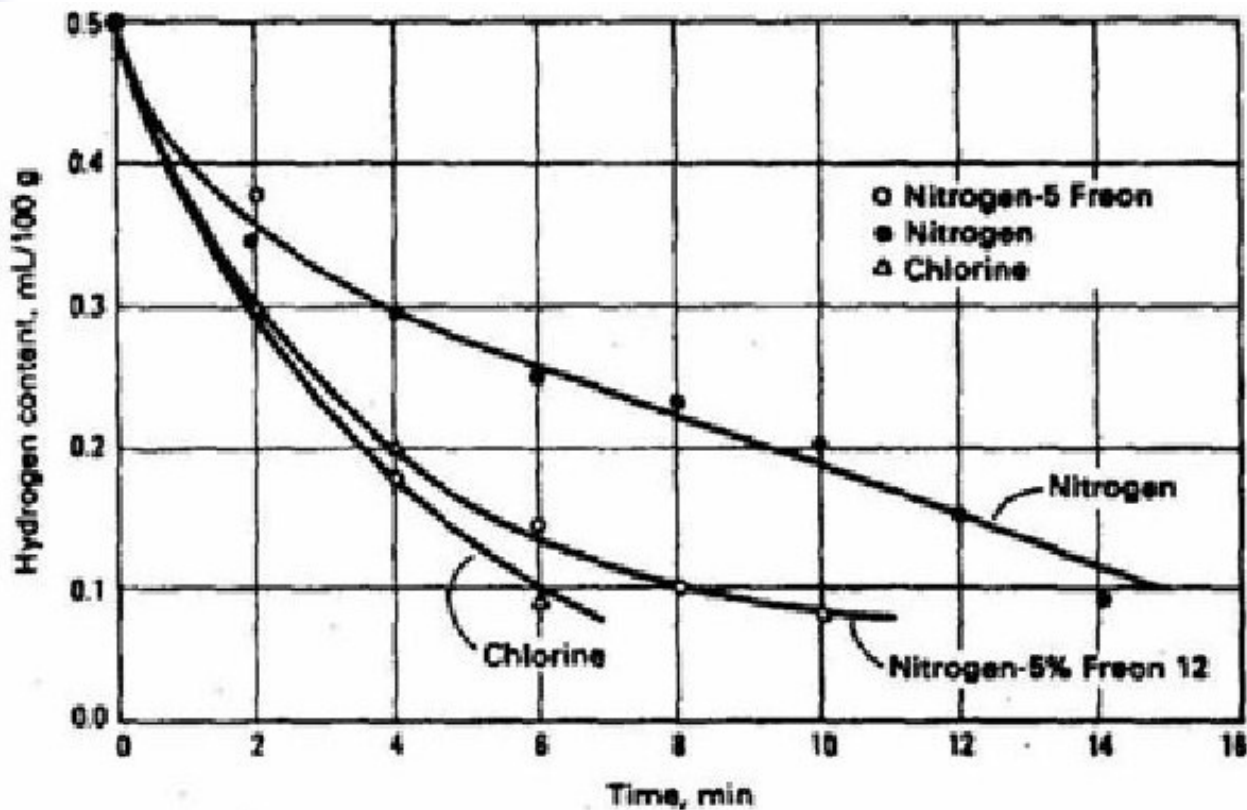
Solubilidade do H no Al

Exemplo: desgaseificação de Al



Esquema de uma unidade de desgaseificação contínua (rotor).

Exemplo: desgaseificação de Al



Redução do teor de H dissolvido no banho com o tempo de desgaseificação.



Bibliografia das Aulas

- GARCIA, Amauri, Solidificação – fundamentos e aplicações, UNICAMP, 2a ed., 2007
- CAMPOS FILHO, Mauricio Prates de e DAVIES, Graeme John. Solidificação e fundição de metais e suas ligas, Rio de Janeiro: Livros Técnicos e Científicos, 1978.
- American Society for Metals. ASM Handbook Committee. Metals Handbook (Casting), 9a ed., vol. 15, Ohio, 1988.
- KALPAKJIAN, Serope e SCHMID, Steven. Manufacturing processes for engineering materials, 5a ed., Pearson Education, New Jersey, 2007.
- CAMPBELL, John, Castings, Elsevier, Oxford, 2ª ed., 2004.
- CAMPBELL, John, Castings practice – the 10 rules of castings, Elsevier, Oxford, 2004.